University of Alberta

Characterization of ZrO_2-MoO_3 Catalysts

By
Carolyn Dawn Kenney

A thesis submitted to the Faculty of Graduate Studies and Research in partial fulfillment of the requirements for the degree of Master of Science

in
Chemical Engineering

Department of Chemical & Materials Engineering

Edmonton, Alberta
Fall, 2004

Library and Archives Canada

Published Heritage Branch

395 Wellington Street
Ottawa ON K1A 0N4
Canada

Bibliothèque et Archives Canada

Direction du Patrimoine de l'édition

395, rue Wellington
Ottawa ON K1A 0N4
Canada

Your file Votre référence
ISBN: 0-612-95782-9
Our file Notre référence
ISBN: 0-612-95782-9

The author has granted a non-exclusive license allowing the Library and Archives Canada to reproduce, loan, distribute or sell copies of this thesis in microform, paper or electronic formats.

The author retains ownership of the copyright in this thesis. Neither the thesis nor substantial extracts from it may be printed or otherwise reproduced without the author's permission.

L'auteur a accordé une licence non exclusive permettant à la Bibliothèque et Archives Canada de reproduire, prêter, distribuer ou vendre des copies de cette thèse sous la forme de microfiche/film, de reproduction sur papier ou sur format électronique.

L'auteur conserve la propriété du droit d'auteur qui protège cette thèse. Ni la thèse ni des extraits substantiels de celle-ci ne doivent être imprimés ou aturement reproduits sans son autorisation.

In compliance with the Canadian Privacy Act some supporting forms may have been removed from this thesis.

While these forms may be included in the document page count, their removal does not represent any loss of content from the thesis.

Conformément à la loi canadienne sur la protection de la vie privée, quelques formulaires secondaires ont été enlevés de cette thèse.

Bien que ces formulaires aient inclus dans la pagination, il n'y aura aucun contenu manquant.

Canada

To my parents, Don and Joan, my brothers, David and Brian, and my sister, Nicole.

ACKNOWLEDGEMENTS

There are many people that have made the completion of this degree possible. I am extremely grateful for the support that I received from my parents, Don and Joan Kenney, my sister, Nicole, and my brothers, David and Brian. I would like to acknowledge my supervisor, Dr. Nelson, for his tremendous help and encouragement. I would like to thank everyone in the group for their help and friendship, with a special thanks to Khanh Tran, Wa'el Abdallah, Zhenhui Wang, and Mingyong Sun. I am thankful for the time and assistance given to me by Andrée Koenig, Walter Boddez, Richard Cooper, Jack Gibeau, and Bob Barton. The financial support of Syncrude Canada Ltd., Natural Sciences and Engineering Research Council (NSERC), and the Canada Foundation for Innovation is also acknowledged. Last but by no means least, I thank Dr. Maham for his continual encouragement, guidance, and generosity.

TABLE OF CONTENTS

CHAPTER 1 INTRODUCTION
1.1 Aromatic Reduction in Diesel Fuels.....1
1.2 Conventional Hydrotreating Catalysts.....2
1.3 MoO_3-ZrO_2 Catalysts.....2
1.4 Catalyst Characterization.....4
1.5 Objective of Study.....4
1.6 Hypothesis of Study.....5

CHAPTER 2 LITERATURE REVIEW
2.1 Cetane Improvement of Diesel Fuels.....6
2.2 Ring-Opening of Model Compounds with Conventional Hydrotreating Catalysts.....7
2.2.1 Monofunctional Catalysts.....7
2.2.2 Bifunctional Catalysts.....8
2.3 MoO_3-ZrO_2 catalysts.....11
2.3.1 Preparation of MoO_3-ZrO_2 Catalysts.....11
2.3.2 Crystalline Structure.....12
2.3.3 Surface Area.....13
2.3.4 Reducibility.....13
2.3.5 Acidity.....14
2.4 Reaction of Model Compounds with MoO_3-ZrO_2 Catalysts.....15
2.5 Methyl-Cyclopentane as a Probe Molecule.....17
2.6 Noble Metals.....18
2.7 Summary.....19

CHAPTER 3 EXPERIMENTAL METHODS
3.1 Introduction.....20
3.2 Materials and ZrO_2-MoO_3 Catalyst Synthesis.....20
3.2.1 Chemicals.....20
3.2.2 Catalyst Preparation.....21
3.3 X-Ray Photoelectron Spectroscopy (XPS).....22
3.3.1 AXIS HSi 165 XPS Analysis System.....23
3.3.2 XPS Sample Preparation.....24
3.4 X-Ray Diffraction (XRD).....24
3.4.1 Philips PW 1730/10 X-Ray Diffractometer.....25
3.5 CO_2 Adsorption.....25
3.5.1 Setaram Differential Scanning Calorimeter DSC 111.....26
3.5.2 CO_2 Sorption Experimental Procedure.....27
3.6 Brunauer-Emmett-Teller (BET) Surface Area Analysis.....29
3.6.1 Autochem II 2920 Automated Catalyst Characterization System.....30
3.6.2 Autochem II 2920 Sample Introduction.....31
3.6.3 BET SA Experimental Procedure.....33
3.6.4 Gas Calibration.....33
3.7 Temperature Programmed Reduction (TPR)/Temperature Programmed Oxidation (TPO).....34

3.7.1 TPR Experimental Procedure.....34
3.7.2 TPO Experimental Procedure.....34
3.8 Temperature Programmed Desorption (TPD).....35
3.8.1 TPD Experimental Procedure.....36
3.9 Ring-Opening Reaction.....36
3.9.1 Ring Opening Reaction Procedure.....37
3.9.2 Dycor Quadrupole Gas Analyzer.....38

CHAPTER 4 RESULTS
4.1 Elemental Compositional Analysis (XPS).....39
4.2 Crystalline Structure (XRD).....41
4.3 CO_2 Sorption (DSC).....45
4.4 BET Surface Area.....48
4.5 Temperature Programmed Reduction (TPR).....51
4.6 Temperature Programmed Oxidation (TPO).....57
4.7 Temperature Programmed Desorption (TPD).....59
4.8 Ring-Opening Reaction.....60

CHAPTER 5 DISCUSSION
5.1 Elemental Compositional Analysis (XPS).....66
5.2 Crystalline Structure (XRD).....67
5.3 CO_2 Sorption (DSC).....70
5.4 BET Surface Area.....70
5.5 Temperature Programmed Reduction (TPR).....73
5.6 Temperature Programmed Oxidation (TPO).....76
5.7 Temperature Programmed Desorption (TPD).....77
5.8 Ring-Opening Reaction.....79

CHAPTER 6 CONCLUSION
6.1 Conclusion.....82
6.2 Future Work.....83

REFERENCES.....85

LIST OF TABLES

CHAPTER 3

3-1 Kratos Analytical Axis 165 XPS Operating Parameters.....23
3-2 Philips PW 1730/10 XRD Operating Parameters.....25

CHAPTER 4

4-1 Predicted and experimental XPS data.....40
4-2 X-Ray Diffraction Lattice Parameters.....45
4-3 Heat of adsorption of the first and third experiment of MoO_3/ZrO_2 catalysts.....48
4-4 Effect of the Mo/Zr ratio on the BET surface area.....49
4-5 BET surface area for different methods of MoO_3-ZrO_2 preparation techniques...50
4-6 Effect of Mo/Zr atomic ratio on H_2 uptake per g_{cat}.....54
4-7 TPR results prior to and following treatment with TPO.....57
4-8 Conversion of methyl-cylcopentane based on data for m/z = 56.....64

LIST OF FIGURES

CHAPTER 3

3-1 Schematic of the DSC 111 silica reactor vessel.....28
3-2 Schematic of the Autochem quartz sample tube.....32

CHAPTER 4

4-1 XRD pattern of molybdenum-zirconium oxides. The dotted lines represent a standard cubic reference pattern (JCPDS file no. 27-997) for cubic ZrO_2.....43
4-2 Monoclinic (a), tetragonal (b), and cubic (c) crystalline structures.....44
4-3 CO_2 adsorption of MoO_3-ZrO_2 catalysts.....46
4-4 TPR profiles of MoO_3-ZrO_2 catalysts.....53
4-5 Variation of total hydrogen uptake with Mo-loading, per m^2_{cat}.....55
4-6 Variation of total hydrogen uptake with Mo-loading, per g_{cat}.....56
4-7 TPO profiles of MoO_3-ZrO_2 catalysts.....58
4-8 Ammonia TPD profiles of MoO_3-ZrO_2 catalysts.....61
4-9 Volume of NH_3 desorbed per unit mass of MoO_3-ZrO_2 catalysts.....62
4-10 Volume of NH_3 desorbed per unit surface area of MoO_3-ZrO_2 catalysts.....63

CHAPTER 1: INTRODUCTION

1.1 Aromatic Reduction in Diesel Fuels

Synthetic crude derived from bitumen and heavy oil residue contains significant quantities of complex aromatic and naphthenic hydrocarbon structures. According to McVicker et al. (2002), petroleum distillates are a complex mixture of five and six membered naphthenes containing multiple alkyl substituents which are joined or fused to each other. Albertazzi et al. (2003) states that straight-run stocks typically contain 20-40 vol.% aromatics while cracked stocks contain 40-70 vol.%. These naphthenic and aromatic rings must be selectively opened to obtain diesel fuels with high cetane numbers, giving shorter ignition delays, smoother engine operation, more complete combustion, better startability, and less particulate in the exhaust gases (Corma et al., 2001 and Albertazzi et al., 2003).

Increasing the cetane number involves converting ring compounds to straight chain paraffins and olefins over bifunctional or monofunctional catalysts. Over bifunctional catalysts, six-membered rings are isomerized to five membered rings over an acidic function (McVicker et al., 2002). The five-membered rings are selectively opened over a metal function, yielding linear paraffins and olefins. A balanced acidic and metallic functionality is essential to produce linear alkanes without significant dealkylation. Reactions occurring over monofunctional catalysts proceed via a non – classical Haag-Dessau mechanism, where alkanes are directly protonated to non-classical carbonium ions in the transition state (Weitkamp et al., 2001).

1.2 Conventional Hydrotreating Catalysts

The catalyst properties and requirements for the hydroconversion, or selective ring opening of bitumen derived gas oils, are poorly understood. Conventional supports, such as zeolites, give poor ring-opening selectively. Studies involving zeolites show that pore size effects product distribution. When tetralin is used as a probe molecule over microporous and mesoporous zeolites, compounds with low cetane ratings are produced via cracking of the substituted alkyl groups (Corma et al., 2001). Corma et al. reported a propane yield of 35% over catalysts with a micropore volume of 0.12 cm^3/g and a Si/Al molar ratio of 15. Reducing the micropore volume to 0.09 cm^3/g and increasing the Si/Al ratio to 80 decreased the production of propane by 15% and increased the production of butyl-benzene by 15%, which resulted in a cetane rating increase from 0 to 15. This slight improvement in cetane rating still does not meet anticipated cetane rating specifications of > 40.

Better selectivity towards ring-opening has been obtained over bifunctional catalysts containing solid acids and noble metals. McVicker et al. (2002) has shown that methyl-cyclopentane reacted over 0.9% Ir/Al_2O_3 gives a ring-opening selectivity of 99 % and conversion of 52%. For catalysts containing 0.6% Pt/SiO_2, 0.3% Pt/Al_2O_3, and 15% Ni/Al_2O_3, the selectivity towards ring-opening was greater than 80%, but the maximum conversion was only 24% (McVicker et al., 2002).

1.3 MoO_3-ZrO_2 Catalysts

Maity et al. (2000) does not predict further improvement of conventional catalysts but rather the development of new catalysts. ZrO_2 based catalysts have been gaining

attention because of their high thermal stability, chemical inertness, acidic, basic, and reducing properties (Bhaskar et al., 2001). Reddy et al. (2000) has reported that ZrO_2 has a melting point of 2973 K, a low thermal conductivity, and a high resistance for corrosion. Some reactions in which ZrO_2 has been used as a catalyst support or catalyst include the hydrogenation of CO, olefins, and dienes, and acid catalyzed reactions such as cracking, alkylation, isomerization, and condensation.

By itself, ZrO_2 does not have superior catalytic properties. Various studies have reported that pure ZrO_2 has a low surface area (42 – 96 m^2/g, Calafat et al., 2000 and Zhao et al., 1997), is not reducible up to 1000°C (Bhaskar et al., 1997), and exists in the monoclinic phase (Calafat et al., 2000). To improve the catalytic properties of ZrO_2, molybdenum is commonly incorporated. Various studies have shown that, depending on the method of preparation, incorporation of molybdenum increases the surface area, enhances the reducibility, and changes the crystalline structure to a more catalytically active form.

According to Calafat et al. (2000), stabilization of the ZrO_2 phase can be done in three different ways: wet-impregnation, sol-gel method, or co-precipitation. Catalysts prepared by different methods of preparation exhibit different properties. One of the catalytic properties that the method of preparation has a significant effect on is the surface area. MoO_3-ZrO_2 catalysts prepared by co-precipitation or the sol-gel method exhibit a maximum surface area (S_{max}) with increasing Mo-loading followed by a decrease in surface area, likely due to the formation of a new Mo phase. Catalysts prepared by wet-impregnation give lower surface areas that decrease with molybdenum loading, owing to blockage by molybdenum oxide (Li et al., 1999 and Maity et al., 1999).

1.4 Catalyst Characterization

In this study, the morphological and thermochemical properties of monofunctional ZrO_2-MoO_3 catalysts with varying Mo loadings are studied. Seven ZrO_2-MoO_3 catalysts with molybdenum loadings from 0 to 19 at. % were prepared by co-precipitation. The morphological and chemical properties of the catalysts were studied using spectroscopic and thermochemical techniques. X-ray photoelectron spectroscopy (XPS), x-ray diffraction (XRD), and BET surface area were used to determine the chemical composition, the crystalline structure, and the surface area of the catalysts. Temperature programmed reduction (TPR), CO_2 sorption, and temperature programmed desorption (TPD) of ammonia were used to characterize the reducibility, the basicity, and acidity of the catalysts. Reaction studies were carried out using methyl-cyclopentane (mcp) as a model compound at 300°C and 0.1 MPa.

The goal of catalyst characterization was to develop correlations between adsorption and reactivity data. Having the ability to predict catalyst activity and selectivity with adsorption data reduces the need for high pressure reactor studies.

1.5 Objective of Study

The objective of this study was to prepare and thermochemically characterize a series of monofunctional MoO_3-ZrO_2 catalysts. Seven catalysts were prepared containing 0, 3, 5, 9, 11, 16 and 19 at. % molybdenum through co-precipitation and calcination at 500°C. Each catalyst was characterized using X-ray photoelectron spectroscopy (XPS), X-ray diffraction (XRD), BET SA, CO_2 isothermal adsorption, temperature programmed

reduction (TPR), and temperature programmed desorption (TPD) of ammonia. Reaction studies were carried out using methyl-cyclopentane as a probe molecule.

1.6 Hypothesis of Study

Based on previous work (Calafat et al., 2000, Bhaskar et al. 2001, and Maity et al., 2000), it is expected that molybdenum will act as a stabilizer when incorporated into ZrO_2. As a result, MoO_3-ZrO_2 catalysts are expected to exist in the metastable cubic or tetragonal phase, to have a higher surface area, and to be more easily reduced. With regards to activity and selectivity, it is expected that modifying the crystallite structure, increasing the surface area, and improving the reducibility through incorporation of molybdenum will enhance the catalyst activity and selectivity towards n-alkanes.

CHAPTER 2: LITERATURE REVIEW

2.1 Cetane Improvement of Diesel Fuels

Traditionally, aromatic compounds have been used as octane boosters in gasoline fuel (Berger et al., 2003, Raichle et al., 2002, and Weitkamp et al., 2001). Because of new legislation set by the European Auto Oil Programme and other organizations around the world, aromatics are becoming less desirable for this purpose (Berger et al., 2003). Weitkamp et al. (2001) estimated that in 1999, Western Europe produced 6.9 Mt benzene, 2.3 Mt toluene, and 1.9 Mt xylenes. Currently, extensive work is being done to convert excess aromatics to high quality synthetic steamcracker feed (ethane, propane, and n-butane) and to cleaner distillate streams for the production of diesel fuels.

Diesel fuels that contain high concentrations of aromatics have poor cetane numbers. Cetane numbers are assigned to fuels based on their ability to burn, which is governed by their delay during ignition (Corma et al., 2001). The cetane scale is based on the compound n-hexadecane, or cetane, which has a cetane number of 100 owing to its short ignition delay (Corma et al., 2001). Other compounds, such as tetralin and heptamethylnonane have cetane values of 0 and 15, respectively (Corma et al., 2001).

Efforts to improve the cetane quality of diesel fuels involve hydrotreatment over monofunctional or bifunctional catalysts, yielding paraffins, olefins, and alkyl-substituted rings. Ring-opening reactions over monofunctional catalysts proceed via the Haag-Desau mechanism, where alkanes are directly protonated to non-classical carbonium ions in the transition state (Weitkamp et al., 2001). Characteristics of the Haag-Desau mechanism include preferential cracking of the most highly branched carbon and high activation

energies. Weitkamp et al. (2001) observed the Haag-Desau mechanism when different product compositions were observed during hydrocracking of hydrocarbons containing 6-9 carbon atoms. Higher yields of methane, ethane, and butane from benzene were observed at 400°C compared to at 250°C, providing evidence supporting the Haag-Desau mechanism.

Classical bifunctional (or bimolecular) reaction mechanisms have been traditionally reported for the catalytic ring opening of cycloalkanes over solid-acid supported noble metals (McVicker et al., 2002). Reactions over bifunctional catalysts proceed via isomerization of six-membered rings to five membered rings over an acidic function followed by selective ring-opening over a metal function (McVicker et al., 2002). A balanced acidic and metallic functionality is essential to produce linear alkanes without significant dealkylation.

2.2 Ring-Opening of Model Compounds with Conventional Hydrotreating Catalysts

2.2.1. Monofunctional Catalysts

Conventional catalysts show little promise for use in ring-opening reactions. When reacting tetralin over zeolites, 85 % of the total product conversion is made up of C1 to C4 fractions, naphthalene, benzene, and C10 olefin/naphthene aromatics (Corma et al., 2000). The selectivity towards these products depends on the type of zeolite employed. Large pore zeolites give better selectivity towards high molecular weight ring-opening products compared to medium pore zeolites. Carma et al. (2000) demonstrates that ZSM-5 and other medium pore zeolites are not suitable as acid

functions for ring-opening because of their inability to handle polyaromatic and aromatic-naphthenic rings in light cycle oil (LCO) and their tendency to promote dealkylation. Propene and benzene are the primary reactant products formed with ZSM-5 (medium pore zeolite) at 450°C. Marginal improvement is observed for the ring opening of aromatic-naphthenic condensed rings using large-pore zeolites (USY or Beta zeolite). However, they both show an initial molar selectivity of less than 1 % towards C6 aliphatics for reaction at 450°C.

Studies using decalin as a probe molecule also indicate that large pore zeolites are more effective at producing high molecular weight ring-opening products. The primary products observed during the cracking of decalin are gaseous molecules, C6 naphthenics, and C10 aromatics (Corma et al., 2000). Zeolites containing large sized pores (Beta zeolite) produce less gaseous molecules than zeolites containing medium sized pores (ZSM-5). Nevertheless, Beta zeolite only gives an initial molar selectivity of 7 % towards C6 aliphatics (Corma et al., 2000).

Numerous studies involving hydrogenolysis over solid acids for the production of synthetic steamcracker feedstock (ethane, propane, and n-butane) have been conducted (Berger et al., 2003 and Raichle et al., 2002). Producing steamcracker feed involves hydrogenation of aromatics to cycloalkanes followed by hydroconversion into C_{2+}alkanes. Berger et al. (2003) reports selectivities of methyl-cyclohexane to C_{2+}n-alkanes of 10% (H-Y, large pore zeolite), 28% (H-ZSM-5, medium pore zeolite), and 64% (H-ZSM-22, medium pore zeolite). These results are consistent with what has been reported by Raichle et al. (2002). Raichle et al. (2002) reports that ZSM-5 and ZSM-11 (medium pore zeolite) with a 3-D pore system are the best at converting cyclohexane to

C_{2+}n-alkanes. A 70 % conversion of methyl-cyclohexane to ethane, propane, and n-butane without significant amounts of methane (4 %) is observed for H-ZSM-5. Berger et al. (2003) attributes the dependence of product distribution on the pore size to the transition state of bimolecular cracking (leading to branched alkanes instead of n-alkanes), which is hindered in the pores of medium pore zeolites (Berger et al., 2003).

2.2.2 Bifunctional Catalysts

McVicker et al. (2002) studied metal-catalyzed hydrogenolysis for the selective ring-opening of naphthenic compounds. Reactions were carried out in a 25 cm^3 stainless-steel, fixed-bed, downflow reactor with an operating capacity of 5500 kPa and 550°C. Catalysts were prepared by incipient wetness of well-characterized supports (SiO_2, Al_2O_3, USY (Si/Al = 37), and ECR-32) with metal solutions containing Pt, Ni, Ru, or Ir. Some of the model compounds investigated include methyl-cyclopentane and methyl-cyclohexane.

Of the catalysts tested with methyl-cyclopentane (Pt/SiO_2, Pt/Al_2O_3, Ni/Al_2O_3, Ru/SiO_2, Ir/Al_2O_3), Ir/Al_2O_3 gives the highest conversion (52 %) and ring-opening yield (99 %). Although this ring-opening yield is high, the overall conversion and selectivity towards n-hexane is unacceptably low. McVicker et al. (2002) speculates that ring-opening with Ir/Al_2O_3 proceeds via a non-selective, dicarbene mechanism, based on the hydrogenolysis product distribution (n-hexane <1% , 2-methylpentane = 70%, 3-methylpentane = 29%).

Conversion and ring-opening selectivity values are even lower when methyl-cyclohexane is used as a model compound. The highest ring-opening activity is observed

for Ir/Al_2O_3 (87 %), but the overall conversion is low (14.5 %). Ru/SiO_2 catalysts give higher conversion (52.9 %) but with reduced ring-opening selectivity (4 %). As is the case for methyl-cyclopentane, McVicker et al. (2002) concludes that reaction with methyl-cyclohexane proceeds via a dicarbene mechanism, adding that flat adsorption of a cyclohexyl ring is not favorable. McVicker et al., (2002) attributes differences in ring-opening selectivities and conversions between methyl-cyclopentane and methyl-cyclohexane to the higher ring stain present in five-membered rings compared to six-membered rings.

McVicker et al. (2002) attests that improving the selective ring-opening of six-membered rings can be achieved by adding an acidic function that will first isomerizes the six-membered ring to a five-membered ring. When 2 % Ir/Al_2O_3 is admixed with 0.9 % Pt/USY (Si/Al = 37, low to moderate acid strength), a conversion of 55 % and ring-opening yield of 70 % was observed.

The hydrogenolytic ring opening capability of Rh/Al_2O_3 catalysts as a function of hydrogen pressure and temperature was investigated by Teschner et al. (2000) using methyl-cyclopentane as a probe molecule. The reactions were carried out in a closed-loop apparatus at 120 - 480 Torr and 195 – 240°C. Three different Rh/alumina catalysts were prepared containing 0.3 %, 3 %, and 10 % Rh on an Al_2O_3 support by wet-impregnation followed by reduction in H_2 at 300 (LTR) or 700°C (HTR).

Teschner et al. (2000) observed a monotonic increase in ring-opening activity with increasing H_2 pressure for catalysts containing 0.3% Rh (LTR and HTR). The highest and lowest ring-opening activities were observed for catalysts containing 10 % Rh (LTR) and 3 % Rh (LTR), respectively. Catalysts containing 10 % Rh (LTR and

HTR) and 3 % Rh (LTR and HTR) have selectivities towards <C6 fragments that are independent of the hydrogen pressure, whereas catalysts containing 0.3% Rh (LTR and HTR) show a monotonic increase in selectivity towards <C6 fragments with increasing H_2 pressure. Teschner et al. (2000) attributes these variations in ring-opening selectivity to the different particle morphologies present for different metal loadings and treatment temperatures.

2.3 MoO_3-ZrO_2 catalysts

Improvement of conventional hydrotreating catalysts has mainly leveled off (Maity et al., 2000). Much emphasis is now being placed on the development of new catalysts. ZrO_2 is gaining attention as a catalyst support because of its strong interaction with active phases, its reducing and oxidizing abilities, its acidic and basic functionality, and its thermal and chemical stability (Bhaskar et al., 2000). Typically, metal oxides (MoO_3-, WO_3-, or CuO-) are incorporated with ZrO_2 to further improve its catalytic properties (Calafat et al., 2000).

2.3.1 Preparation of MoO_3-ZrO_2 Catalysts

The addition of metal oxides to stabilize ZrO_2 can be done in three different ways: (i) wet-impregnation through coating of ZrO_2 with a second oxide, (ii) sol-gel impregnation with a second oxide, and (iii) co-precipitation of solid-precursors. Different catalytic properties are achieved based on the method of preparation.

2.3.2 Crystalline Structure

Various studies show that pure ZrO_2 exists primarily in the monoclinic phase with a fraction existing in the tetragonal phase (Bhaskar et al., 2000 and Maity et al., 1999). Stabilization of ZrO_2 in the cubic or tetragonal phase can be achieved through the addition of molybdenum, which reduces the zirconia grains below a certain size and retards the grain growth rate. Calafat et al. (2000) observes that MoO_3-ZrO_2 catalysts prepared by co-precipitation and calcined at 500°C required 10 – 50 at. % molybdenum for stabilization in the tetragonal phase. Zhao et al. (1997) observes a phase transition from monoclinic to tetragonal at Mo-loadings between 3 – 14 at. % for catalysts prepared by hydrogel impregnation and calcined at 450°C. Xie et al. (2000) reports that catalysts prepared by wet impregnation and calcined between 500 - 700 °C exhibit a phase transition from monoclinic to tetragonal at 9 at. % molybdenum.

The formation of a new molybdenum phase at high Mo-loadings has been reported in several studies. Calafat et al. (2000) speculates the formation of a new Mo-Zr for catalysts containing 50 at. % molybdenum through comparison of their XRD pattern with the JCPDS Powder Diffraction File for $Zr(MoO_4)_2$. Additional evidence supporting the existence of a new molybdenum phase is the appearance of a third reduction peak in the TPR profiles (Calafat et al., 2000).

2.3.3 Surface Area

The effect of molybdenum loading on the surface area of MoO_3-ZrO_2 catalysts depends on a number of factors, including the method of preparation and the calcination temperature. Surface area values of 42 m^2/g (Calafat et al., 2000) and 84 m^2/g (Bhaskar

et al., 2001) are reported for pure zirconia calcined at 500°C. Catalysts prepared by co-precipitation or sol-gel impregnation have surface areas that increase with molybdenum loading to a maximum value (S_{max}) and then decrease (Calafat et al., 2000 and Zhao et al., 1997). Calafat et al. (2000) reports that the addition of 20 and 10 at. % molybdenum gives S_{max} values of 116 and 89 m^2/g after calcination at 500 and 600°C. S_{max} values of 224 and 189 m^2/g after calciniation at 550 and 600°C (Mo/Zr = 0.22) are reported by Zhao et al. (1997). According to Calafat et al. (2000), incorporation of molybdenum increases the surface area by decreasing the sintering and grain-growth rate of ZrO_2. After S_{max}, the drop in surface area is attributed to the formation of a new MoO_3 phase, as indicated by the XRD profiles. MoO_3-ZrO_2 catalysts prepared by wet impregnation give surface areas that decrease with Mo-loading (Li et al., 1999 and Maity et al., 1999). Maity et al. (1999) speculates that low surface areas are observed because of blockage of the pore mouth with MoO_3.

2.3.4 Reducibility

TPR is widely used for screening catalyst preparation and regeneration techniques (Jones, 1986). Jenkins developed the technique in the 1970's, which involves flowing a hydrogen gas mixture over a solid while heating it at a linear rate (Jones, 1986). The appearance of TPR profiles is highly dependent on the heating rate, where higher heating rates give higher peak temperatures and better resolution.

High hydrogen uptakes at low temperatures are desired, since reduction is used to activate catalysts. Combining MoO_3 with ZrO_2, through wet-impregrenation or co-precipitation gives catalysts that are more reducible. Maity et al. (1999) reports that pure

zirconia is not reducible up to 726°C. With the addition of molybdenum through wet-impregnation, Bhaskar et al. (2001) states that the reducibility of MoO_3-ZrO_2 catalysts improves and occurs in two stages. First, reduction of MoO_3 to MoO_2 occurs at around 767°C followed by reduction of MoO_2 to Mo at around 987°C. Calafat et al. (2000) observes two reduction peaks at 416 and 660°C for catalysts prepared by co-precipitation, attributing them to the reduction of dispersed polymolybdates followed by the reduction of MoO_3 to MoO_2.

2.3.5 Acidity

The activity and selectivity of metal oxides is related to their acidic and basic functionality (Auroux et al., 2001). Numerous investigators report that the catalyst activity and selectivity increases with increasing surface acidity. Baskar et al. (2001) states that as the number of strong acid sites increases, the conversion of 3-picoline and the selectivity towards nicotinonitrile increases over MoO_3-ZrO_2 catalysts. Li et al. (1999) reports that the esterfication over MoO_3-ZrO_2 increases with increasing acidity.

Two techniques that are used to test the acidity of solids are the indicator titration method and the gas-phase adsorption method (Carniti et al., 1994). The gas-phase adsorption method is more commonly employed because both Bronsted and Lewis sites can be investigated, different probe molecules can be used, and information about the strength and quantity of acid sites can be obtained. Ammonia is commonly used as a probe molecule because of its stability, small size, and strong basic strength.

The peak temperature of NH_3 desorption can be used to compare the strength of different acids. Compared to other solid acids, MoO_3-ZrO_2 catalysts are relatively weak

(Li et al., 1999). Li et al. (1999) lists peaks of NH_3 desorption at 200°C (ZrO_2 prepared by impregnation of $Zr(OH)_4$ and calcined at 300-900°C), 327°C (SiO_2-Al_2O_3), 377°C (H-ZSM-5), 427°C (mordenite) and 557°C ($Cs_{2.5}H_{0.5}PW_{12}O_{40}$). Bhaskar et al. (2001) reports two peaks at slightly higher temperatures, 300 and 550°C, for ZrO_2 catalysts prepared by incipient wetting of ZrO_2.

2.4 Reaction of Model Compounds with MoO_3-ZrO_2 Catalysts

MoO_3-ZrO_2 catalysts have been extensively characterized, both morphologically and thermochemically, but limited data regarding their selectivity and activity towards ring-opening exists. Reaction studies involving MoO_3-ZrO_2 catalysts include ammoxidation of 3-picoline to nicotinonitrile (Bhaskar et al., 2000), esterfication of acetic acid with ethanol, dehydration of 2-butanol in the presence of water vapor (Li et al., 2002), hydrodesulfurization (HDS) of thiophene, hydrogenation (HYD) of cyclohexene, hydrodeoxygenation (HDO) of tetrahydrofuran (Maity et al., 1999), and hydrolysis of ethyl acetate in excess water (Li et al., 1999).

Bhaskar et al. (2000) investigated the catalytic properties of MoO_3-ZrO_2 catalysts (prepared by incipient wetting of ZrO_2 and calcined at 500°C) in the conversion of 3-picoline to nicotinonitrile. The reactions were carried out in a down flow fixed bed reactor operating at atmospheric pressure and at temperatures ranging from 300 to 550°C. The selectivity towards nicotinonitrile increased with molybdenum loading up to 7 wt. % molybdenum and then remained constant, whereas the conversion increased up to 7 wt. % molybdenum and then decreased. Bhaskar et al. (2001) concludes that a highly dispersed

molybdenum phase at low Mo-loadings is responsible for the conversion of 3-picoline to nicotinonitrile.

Esterfication of acetic acid with ethanol was carried out in a three-necked flask at 70°C by Li et al. (2002). 0.8 g of MoO_3-ZrO_2 catalyst (prepared by impregnation of $Zr(OH)_4$ with $(NH_4)6Mo_7O_{24}{\cdot}4H_2O$ and calcination at 200 – 800°C), 1 cm^3 acetic acid (17 mmol), 1 cm^3 ethanol (17 mmol), and 5 cm^3 toluene were used in each reaction. For the dehydration of 2-butanol in the presence of water vapor, a flow reactor operating at 150°C and atmospheric pressure was used. In both reactions, MoO_3-ZrO_2 catalysts give higher conversion values (esterfication = 48.9 %, dehydration = 99.7 %) compared to other catalysts such as MoO_3/TiO_2, WO_3/ZrO_2, SiO_2-Al_2O_3, and H-ZSM-5. In the case of the dehydration of 2-butanol, the conversion increased with calcination temperature up to 600°C and then decreased.

The hydrodesulfurization (HDS), hydrogenation (HYD), and hydrodeoxygeneration (HDO) activities of MoO_3-ZrO_2 catalysts (prepared by incipient impregnation of a commercial zirconia support and calcination at 450°C) were investigated by Maity et al. (1999). The reactions were carried out at 400°C and atmospheric pressure with sulfided catalysts. For all three reactions, the activity increases with Mo-loading up to 6 wt. % and then decreases. The quasi turnover (ratio of moles of reactant reacting per hour per gram of molybdenum) frequencies are practically constant with Mo-loading up to 6 wt. % and then start to decrease. Compared to MoS_2/Al_2O_3 catalysts, better HDS activity of MoS_2/ZrO_2 catalysts is observed.

The hydrolysis of ethyl acetate over MoO_3-ZrO_2 catalysts (prepared by impregnation (Imp) of $Zr(OH)_4$ or co-precipitation (Pre) and calcination at 200 – 1000°C)

was carried out in a batch reactor at 70°C by Li et al. (1999). A 5 wt % solution of ethyl acetate (30 cm^3, 17 mmol) along with 0.8 g of solid catalyst was used in each reaction. After 2 h of reaction, the conversion increases with Mo-loading up to 20 at. % (Imp) and 10 at. % (Pre) for catalysts calcined at 800°C. When catalysts containing 9 at. % molybdenum (Imp) are calcined at temperatures from 200 to 1000 °C, the conversion increases to 500°C and then decreases. After carrying out various surface characterization techniques, Li et al. (1999) attributes the enhanced activity of MoO_3-ZrO_2 catalysts to the increased surface hydrophobicity and acidity brought on by thermal treatment.

2.5 Methyl-Cyclopentane as a Probe Molecule

Ring-opening of model compounds is useful for studying reaction mechanisms before complex feed stocks are used. Probe molecules containing 5 or 6 membered rings are suitable because petroleum distillates contain a complex mixture of five and six membered naphthenes (McVicker et al., 2002). Methyl-cyclopentane (mcp) is widely used as a probe molecule because it can undergo a variety of reaction pathways on different catalysts (Alvarez et al., 1996). According to Zhuang et al. (1996), mcp can undergo dehydrogenation to methyl-cyclopentene, ring enlargement to cyclohexane or benzene, single C-C bond rupture to cyclopentane, ring opening to 2-methyl pentane, 3-methylpentane, or n-hexane, and hydrogenolysis to $< C_6$ molecules. Zhuang et al. (1996) reports that over tungsten carbide, methylcyclopentene and benzene are the main reaction products. According to Alvarez et al. (1996), Pd_n clusters supported over Y zeolite favors mcp ring opening, whereas $[Pd_nH]^+$ favors mcp ring-expansion.

In addition to having the advantage of producing a variety of reaction pathways, mcp is useful as a probe molecule for gaining information about the effect of catalyst structure on product distribution. Teschner et al. (2000) attributes variations in reaction mechanisms of mcp over Rh/Al_2O_3 catalysts to different particle morphologies. Remarkable changes in product distribution are observed for different metal loadings and pretreatment temperatures, owing to different morphologies of Rh particles. Selective ring-opening of mcp was found to occur on pure metallic sites, especially at lower temperatures. This observation, of selective ring-opening involving a flat-lying intermediate, is in agreement with other studies (Teschner et al., 2003).

2.6 Noble Metals

In the 1970's, studies of several transition metals (Ir, Pt, Pd,and Rh) were conducted to classify their hydrogenolytic activity on C6 hydrocarbons (Teschner et al., 2000). Much work has been done since then, owing to the need for reducing the aromatic content in transportation fuels. Despite what has been done, controversy over which metals are the best suited for hydrogenolytic ring-opening remains.

Albertazzi et al. (2003) reports that mcm-41 catalysts impregnated with 1 % Pt exhibit the best catalytic activity, with high yields of fully hydrogenated and high molecular weight ring-opening products. The order of decreasing hydrogenation activity observed by Albertazzi et al. (2003) is Pt > Rh >> Pd >>> Ru ~ Ir.

In contrast to Albertazzi et al., McVicker et al. (2002) reports that iridium has the highest activity and selectivity for cleaving unsubstituted C-C bonds in five and six-membered rings, adding that the ring-opening rate over iridium is directly proportional to

the number of unsubstituted H_2C-CH_2 bonds. McVicker et al. (2002) attributes the increase in ring-opening rate to a dicarbene reaction mechanism, in which cyclopentyl rings bond perpendicularly to the iridium surface. Pt, on the other hand, adsorbs cyclopentyl rings parallel to the metal surface (McVicker et al., 2002).

In addition to the type of metal, the metal loading and method of preparation have a marked effect on ring-opening activity. Teschner et al. (2000) compares catalysts containing 0.3, 3, and 10 % Rh prepared by wet impregnation of Al_2O_3 and reduction at 300 or 700°C. Overall, the hydrogenolysis selectivity towards C6 alkanes increases with increasing metal loading, decreasing reaction temperature, and increasing H_2 pressure. Catalysts containing large Rh particles (10 (LTR), 3 (HTR), and 0.3 (HTR) % Rh) resulting from a combination of metal loading and reduction temperature also show an increase in C6 alkane selectivity. Teschner et al. (2000) notes that these results are consistent for what has been found for Ru.

2.7 Summary

The previous discussion shows that conventional hydrotreating catalysts are not suitable for producing high quality diesel fuels. Conventional hydrotreating catalysts lack activity and selectivity towards high molecular weight alkanes. Better catalysts supports, such as ZrO_2, need to be further explored. Studies involving the characterization of ZrO_2-based catalysts have been done, but much work still needs to be done regarding their ring-opening activity and selectivity.

CHAPTER 3: EXPERIMENTAL METHODS

3.1 Introduction

The morphological and chemical properties of ZrO_2-MoO_3 catalysts were investigated using thermochemical and spectroscopic techniques. X-ray photoelectron spectroscopy (XPS), x-ray diffraction (XRD), and BET surface area were used to determine the chemical composition, the crystalline structure, and the physical properties of the catalysts, respectively. Temperature programmed reduction (TPR), CO_2 sorption, and temperature programmed desorption (TPD) were used to characterize the reducibility, the basicity, and acidity of the catalysts. All of these techniques, with the addition of the catalyst preparation technique, are described in the following sections.

3.2 Materials and ZrO_2-MoO_3 Synthesis

3.2.1 Chemicals

1. Ammonium heptamolydate from Fisher Scientific, certified A.C.S grade.
2. Zirconyl chloride octahydrate from Sigma Aldrich, 98% pure.
3. Ammonium hydroxide from Sigma Aldrich, 14.8 M ACS reagent grade.
4. Methyl-cyclopentane from Sigma Aldrich, 97 % pure.
5. Anaerobic carbon dioxide gas from Praxair, 99.99 % pure.
6. Pre-purified argon gas from Praxair, 99.995 % pure.
7. Ultra high purity helium gas from Praxair, 99.999 % pure.
8. 29.9 % nitrogen balance helium gas mixture from Praxair.
9. 14.9 % ammonium balance helium gas mixture from Praxair.

10. 10 % hydrogen balance argon gas mixture from Praxair.

11. 9.87% oxygen balance helium gas mixture from Praxair.

12. Water, purified by reverse osmosis.

3.2.2 Catalyst Preparation

Catalysts were prepared using a technique described by Calafat et al. (2000). ZrO_2-MoO_3 catalysts were prepared by co-precipitation of MoO_3 and ZrO_2 precursors. The solid precursors consisted of zirconyl chloride octahydrate ($ZrOCl_2 \cdot 8H_2O$) and ammonium heptamolybdate ($(NH_4)_6Mo_7O_{24} \cdot 4H_2O$), which were combined to produce various Mo loadings. The amount of $ZrOCl_2 \cdot 8H_2O$ and $(NH_4)_6Mo_7O_{24} \cdot 4H_2O$ required to produce 20 g of each catalyst was calculated using a mole balance. First, the number of moles of Zr was estimated using

$$mol_{Zr} = \frac{20\ g}{MW_{Zr(OH)_4}} \tag{3-1}$$

where $MW_{Zr(OH)_4}$ was 159.25 g/mol. To find the required mass of $ZrOCl_2 \cdot 8H_2O$, the value from Equation 3-2 was multiplied by the molar mass of $ZrOCl_2 \cdot 8H_2O$ (322.3 g/mol). The number of moles of Mo was determined by

$$mol_{Mo} = y * mol_{zr} \tag{3-2}$$

where y was the desired Mo/Zr atomic ratio. The value obtained from Equation 3-2 was divided by 7 and multiplied by the molar mass of $(NH_4)_6Mo_7O_{24} \cdot 4H_2O$ (1235.86 g/mol) to obtain the mass of $(NH_4)_6Mo_7O_{24} \cdot 4H_2O$. In total, seven different catalysts were prepared with Mo/Zr molar ratios of 0.00, 0.02, 0.05, 0.07, 0.10, 0.15, and 0.20.

To prepare the catalyst, $ZrOCl_2 \cdot 8H_2O$ and $(NH_4)_6Mo_7O_{24} \cdot 4H_2O$ were weighed and placed in a 500 mL beaker. Approximately 10 mL of water was added, the solution was stirred, and the contents of the beaker were heated to a maximum temperature of 100°C. Once the solids were completely dissolved, the pH was monitored while ammonium hydroxide was added using a micropipette. When the pH of the solution was 9.25, the solution was vacuum filtered and washed with five parts distilled water. The filter cake was left in the fume hood overnight, dried at 140°C in air for eight hours, and then calcined at 500°C in flowing air for 2 hours. Catalyst samples were placed in a vial and stored in a desiccator for further analysis.

3.3 X-Ray Photoelectron Spectroscopy (XPS)

X-ray photoelectron spectroscopy is used to determine the elemental composition and the oxidation state of a solid surface. When a sample is placed in a vacuum chamber and bombarded with a beam of Al Kα radiation, core and valence electrons are ejected. The kinetic energy of the ejected core electrons is measured and the binding energy is found, according to D. Briggs et al. (1990), using

$$E_k = h\nu - E_B - \phi \tag{3-3}$$

where E_k is the measured kinetic energy (KE), $h\nu$ is the energy of the exciting radiation, E_B is the binding energy of the electron in the solid, and ϕ is the work function. The spectra consist of peaks with varying intensities as a function of binding energy. The peaks are a result of either photoemission from core levels and valence levels or emission of x-ray excited Auger electrons. The binding energy of the core levels reflects the electron structure of the element, as described by D. Briggs et al. (1990). By comparing

the binding energies and the intensity to known standards, the relative surface composition of the solid can be determined.

In this study, XPS was used to verify the Mo/Zr molar ratio in the catalysts, assuming that only ZrO_2 and MoO_3 forms existed. To calculate the Mo/Zr molar ratios, the peaks were identified according to their binding energies using Kratos software. The relative atomic concentration was found by applying relative sensitivity factors to the area of the peaks.

3.3.1 AXIS HSi 165 XPS Analysis System

A Kratos Analytical Axis 165 x-ray photoelectron system, equipped with a spherical sector analyzer, was used to verify the elemental composition of the catalysts. The following settings were used during the analyses:

Table 3-1
Kratos Analytical Axis 165 XPS Operating Parameters

Analyzer Mode	Fixed Analyzer Transmission
Incident Source	Al K_α monochromatic
Source Energy	1486.6 eV
Source Strength	300 W
Pass Energy	160 eV
Dwell Time	0.15 s
Slit Size	800 ×1200 μm
Spot Size	700 × 300 μm
Incident Angle	90°
Step Size	0.5 eV
No. of Scans	2

XPS analyses were performed by Zhenhui Wang and Dimitre Karpuzov.

3.3.2 XPS Sample Preparation

Wafers for XPS analysis were prepared by placing 160 mg of sample into a clean 10 mm dye, inserting a clean 10 mm rod, rotating the rod to spread the powder, and pressing the rod into the dye with a hydraulic press. Each sample was pressed at 15,000 psi for 5 minutes. The wafers were loaded into the loading zone and degassed for approximately 2 hours at $< 5x\ 10^{-9}$ Torr.

3.4 X-Ray Diffraction (XRD)

X-ray diffraction is widely used to characterize the crystalline structure of solid materials, the spacing between crystal planes, and the number of phases present. The technique is based on the constructive interference of diffracted x-rays from the lattice planes of a crystal. When the angle of incidence is equal to the angle of reflection, beam diffraction occurs. In 1912, W.L. Bragg developed a relation between the wavelength of the incident x-ray source, λ, the lattice spacing between the planes in the crystal, d, and the Bragg diffraction angle, θ. According to E. W. Nuffield (1996), this relation is known as Bragg's law and is given by

$$\lambda = 2d \sin\theta \tag{3-4}$$

H.S. Lipson (1970) has stated that, for a cubic crystal, the interplanar spacing, d, and the miller indices, h, k, l are related to the lattice parameter, a, by

$$d = \frac{a}{\sqrt{h^2 + k^2 + l^2}} \tag{3-5}$$

Incident x-rays are created by bombarding copper with high energy electrons. A monochromator is used to filter the K_β rays, which creates its own diffraction pattern and

makes interpretation of the overall diffraction pattern difficult, according to E.W. Nuffield et al. (1996). For powdered samples, the detector is rotated at an angle of 2θ while the source remains fixed. H.S. Lipson (1970) notes that, by rotating the detector, a smooth diffraction pattern is obtained by maximizing the number of crystals orientated for reflection. In this study, the crystalline structure and the lattice parameters were investigated using XRD.

3.4.1 Philips PW 1730/10 X-Ray Diffractometer

The x-ray diffraction spectra were obtained using a Philips PW 1730/10 diffractometer with the following settings:

Table 3-2
Philips PW 1730/10 XRD Operating Parameters

Start Angle	10°	Step Size	0.1° 2θ/step
Stop Angle	80°	Radiation Type	CuK_α
Step Time	10 seconds	Wavelength (λ)	1.541 Å

The diffractometer was equipped with a graphite monochromator to filter the K_β rays. The analog signal was converted to a digital signal via a RS-232 interface and saved on a PC.

3.5 CO_2 Adsorption

Heats of CO_2 adsorption on solid surfaces give information about the strength of basic sites present. According to K. Tanabe (1985), the interaction of acid-base sites on ZrO_2-MoO_3 catalysts plays a role in reactivity. In a calorimetric investigation, CO_2 is dosed onto the catalyst surface at constant temperature while the heat released is

measured by a thermal junction. The heat of adsorption is found by integrating the adsorption peaks that appear in the heat flow spectra.

3.5.1 Setaram Differential Scanning Calorimeter 111

A Tian-Calvet differential scanning calorimeter (DSC) 111 from Setaram was used to study the heat of CO_2 sorption. The calorimeter consisted of three main components: a transducer, a valve cabinet, and controller. The calorimetric transducer was shaped like a rectangular parallelepiped containing two sintered alumina tubes with inner diameters of 7 mm, lengths of 167 mm, and a separation distance of 17 mm. The detection area consisted of a series of Seebeck-effect thermal junctions located in the central 20 mm of the alumina tubes. Heat flow in μV was converted to mW through calibration with a Joule-effect device.

The gas flow rates were controlled by two valves, for the carrier and auxiliary gases, located on the valve cabinet. Upon opening the valves, the pressure gauges above the valves displayed the delivery pressure inside the instrument. Gases were supplied to the instrument by gas supply cylinders set to a delivery pressure of 150 kPa.

A CS 32 controller was used to control the power supply, signal amplification, temperature measurement, temperature regulation, and data collection. Signals were amplified in linear proportion to the heat flux, as described in the *Seteram DSC 111 Operating Manual* (2000), and were converted from analog to digital by the CPU card. The digitized temperature and heat flow signals were transferred from the analyzer to the PC through a RS-232 series interface. Setsoft 2000 software was used to view the data, edit the peaks, and create experimental algorithms.

3.5.2 CO_2 Adsorption Experimental Procedure

For measuring the heat of sorption, the DSC was mounted in the vertical position. A silica reactor vessel, as shown in Figure 3-1, was used to hold the sample. For each analysis, approximately 100 mg of catalyst powder was packed into the silica glass reactor tube. Catalyst particles sticking to the walls of the sample tube above the 12 mm detection area were removed using a brush. The reference and sample tubes were loaded into the calorimetric block by connecting them to the gas inlets at the top of the sample tubes, sliding them into the alumina tubes, and connecting them to the gas outlets. The appropriate 1/8-in diameter metal tubing and Swagelok fittings were used to connect the gases to the instrument. The gas delivery pressure inside the instrument was set to 1 bar by adjusting the valves on the valve cabinet.

The samples were heated to the desired adsorption temperature by ramping the temperature to 100°C, 200°C, or 300°C at a rate of 15°C/min while passing argon (1 L/h). After heating, the temperature was held constant for three hours while the gas was manually switched between argon and carbon dioxide. Argon was passed over the sample for the first 20 minutes of isothermal operation and then replaced by carbon dioxide (1.2 L/h) by shutting the carrier gas valve and opening the auxiliary gas valve. The flow of carbon dioxide was maintained for 20 minutes and then replaced by the flow of argon for 40 minutes. To obtain three data points, the sample was degassed with argon and dosed with carbon dioxide three times. To complete the analysis, the calorimeter was cooled at a ramp rate of 15°C/min under a flow of argon. Cooling water at 18°C circulated throughout the calorimeter block at a flow rate of approximately 2 l/min throughout the entire analysis.

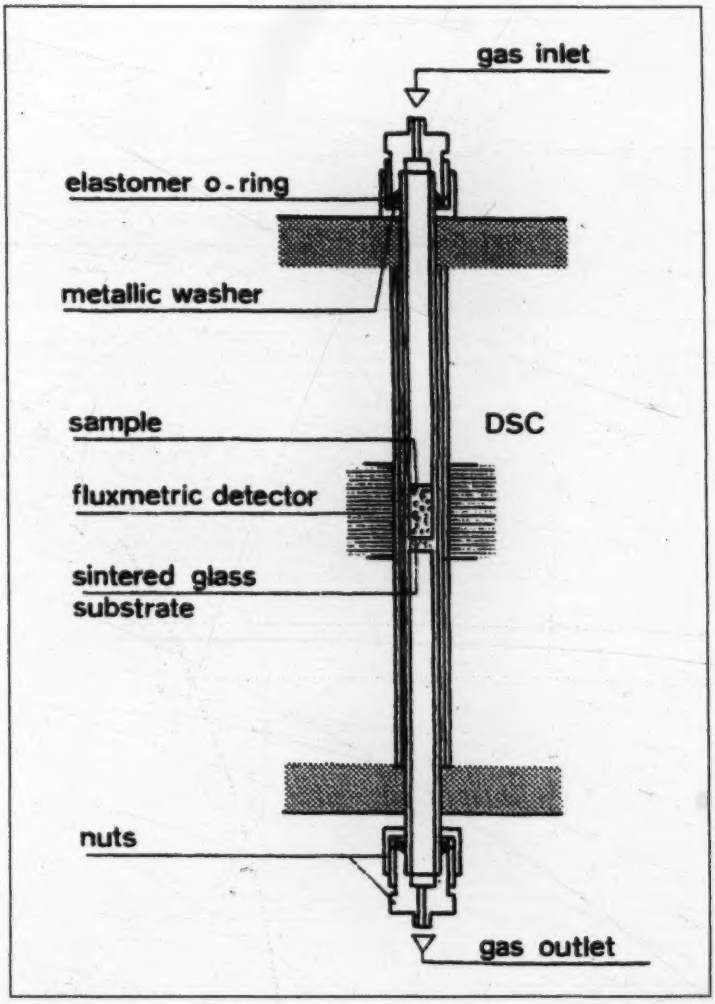

Figure 3-1: Schematic of the DSC 111 silica reactor vessel.

3.6 Brunauer-Emmett-Teller (BET) Surface Area Analysis

The BET surface area technique was developed by Brunauer, Emmett, and Teller in 1945, as stated by G.D. Ulrich (1993). A BET surface area measurement is obtained by adsorbing nitrogen onto a surface at 77 K. After adsorption, the nitrogen is desorbed by rapidly heating the sample to ambient conditions. From the analysis, a plot of nitrogen concentration as a function of time, containing an adsorption and desorption peak, is obtained. By calculating the amount of nitrogen desorbed and knowing the area of nitrogen molecules, the surface area can be determined.

In the present analysis, the BET surface area was calculated using the equations in the *AutoChem II 2920 Automated Catalyst Characterization System Operator's Manual (2003)*:

$$V_{STP} = \frac{V_a}{SW} \times \left(\frac{273.15K}{273.15K + T_a} \right) \times \left(\frac{P_a}{760\,mmHg} \right) \tag{3-6}$$

$$V_m = V_{STP}\left(1 - \frac{P}{P_o}\right) \tag{3-7}$$

$$SA = \frac{V_m}{22414} \times \left(6.023 \times 10^{23}\right) \times A_{N_2} \tag{3-8}$$

where V_a is the volume sorbed at ambient conditions in mL, V_{STP} is the volume sorbed at STP in mL/g of sample, V_m is the volume of the monolayer in mL, T_a is the ambient temperature in K, P is the absolute pressure of N_2 (estimated by % N_2/100 x P_a) in mm Hg, SA is the surface area in m^2/g, A_{N_2} is the surface area of N_2 molecules (0.162 nm^2), SW is the sample weight in g, and P_o is the saturation pressure of N_2 (estimated by P_a + 15 mmHg) in mmHg.

3.6.1 Autochem II 2920 Automated Catalyst Characterization System

An AutoChem II 2920 from Micromeritics was used to perform various temperature-programmed techniques, such as BET surface area, temperature programmed reduction, oxidation, and desorption. The Autochem contained a gold plated thermal conductivity detector, capable of measuring the compositional changes of gases upon interaction with a sample. The amount of power required to maintain the filament at 175°C as the gas flowed past the detector was measured in voltage and recorded at a sampling rate of 1 Hz. The digitized temperature and voltage signals were transferred from the analyzer to the PC with a RS-232 cable. To convert the voltage signal to the amount of gas adsorbed or desorbed, a pulse calibration was done for each analysis gas.

Gas was supplied to the instrument by cylinders equipped with two-stage pressure-reducing regulators set to a delivery pressure of 200 kPa. Copper or stainless steel tubing with a 1/8-in. diameter was used to connect the regulator outlet to the inlet ports on the instrument. Located directly after the preparation, loop, and carrier inlet ports were mass flow controllers. A rotary valve was located after each mass flow controller to direct the flow of the gas. All of these valves were maintained at a temperature of 110°C during operation. After passing through the system, the gas exited through the exhaust ports. If further analysis of the exhaust gas was required, it was connected to a mass spectrometer.

AutoChem II 2920 V2 software was used to create algorithms for setting the gas flow rate and the temperature during an analysis. Gas flow rates from 10 to 75 mL/min and temperatures from –100 to 1100°C were possible.

3.6.2 AutoChem II 2920 Sample Introduction

The same sample preparation technique was used for the BET surface area, the temperature programmed techniques, and the reaction studies. A schematic of the quartz sample tube, along with the pieces that were used for connecting it to the Autochem, is shown in Figure 3-2. About 150 mg of sample was taken in the large arm of the quartz tube on top of a quartz wool plug. After loading the sample, the walls of the sample tube were cleaned with a soft brush, ensuring that the sample was located in the bottom 20 mm of the sample tube, within the heating zone of the instrument.

The sample was connected to the instrument by sliding the sample tube retaining nuts and ferrules over the open ends. A Kalrez® O-ring was placed around the sample tube 1 cm from each opening. The open ends of the sample tube were slid into the openings under the upper panel of the instrument, placing the thermocouple inside the large arm of the sample tube. The fittings were tightened until they were finger-tight. A clamshell-type furnace, equipped with a thermocouple made of Incone^{TM}, was closed around the sample tube.

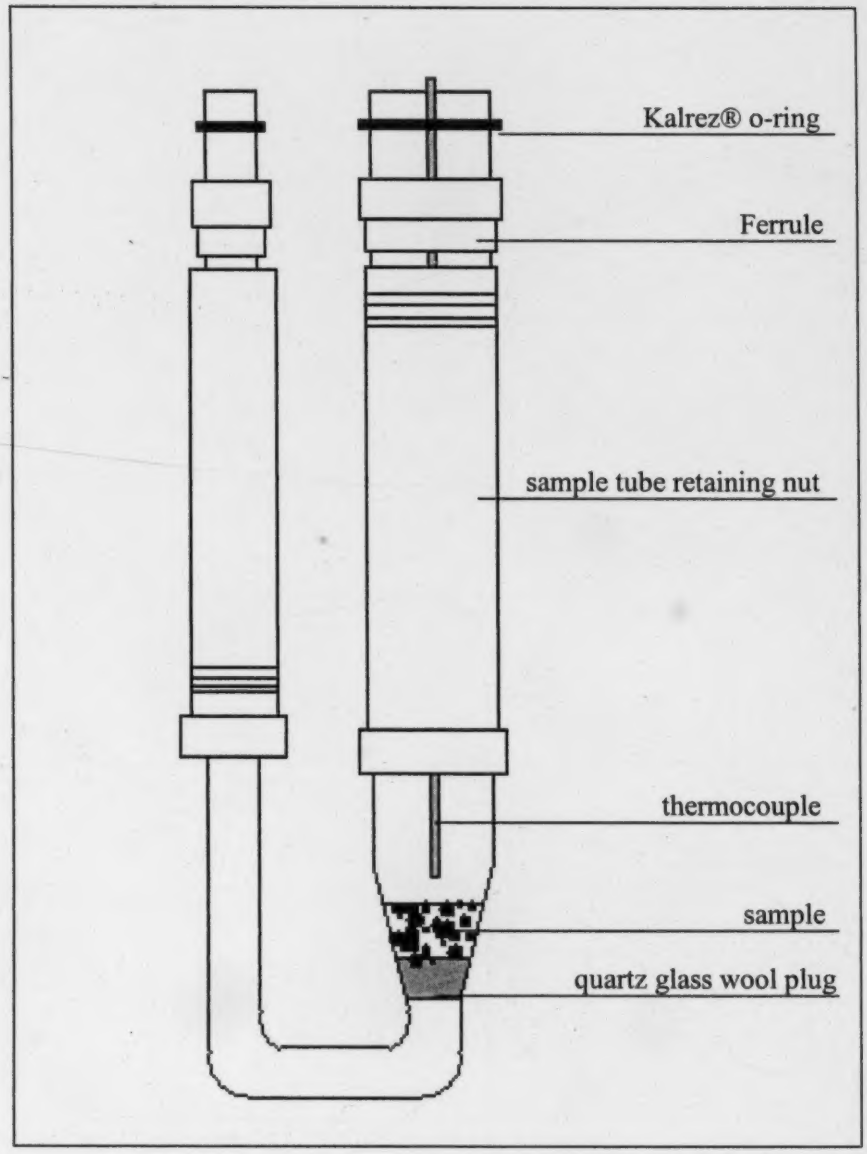

Figure 3-2: Schematic of the Autochem quartz sample tube.

3.6.3 BET Surface Area Experimental Procedure

BET surface area measurements were done using the single point method with an AutoChem II 2920. The sample was pretreated by passing ultra-high pure helium (10 mL/min) while heating from 25°C to 250°C, holding at 250°C for 30 minutes, and cooling to 25°C. The BET surface area was obtained by flowing 29.9% N_2/He (50 mL/min) over the sample, removing the furnace, and immersing the sample tube in a dewar of liquid nitrogen. After 10 minutes, the liquid nitrogen bath was removed and replaced with a dewar of distilled water at room temperature. During the adsorption/desorption process, the thermal conductivity signal was recorded at a rate of 1 Hz. For each sample, the adsorption/desorption process was repeated twice.

3.6.4 Gas Calibration

The Autochem II 2920 was calibrated for each gas to convert the TCD signal from voltage to gas volume. The Autochem II 2920 was equipped with an algorithm for performing gas calibrations. Each calibration was done by installing an empty sample tube and connecting an analysis and inert gas to the analyzer. The proportion of analysis gas was decreased in 10% increments as the amount of inert gas was increased in 10% increments every five minutes while the TCD signal was recorded. Following this procedure, a calibration curve relating the gas concentration to TCD reading was created.

3.7 Temperature Programmed Reduction (TPR) / Temperature Programmed Oxidation (TPO)

Temperature programmed reduction was developed in the mid-70's by Jenkins, according to A. Jones et al. (1986). The technique involves flowing a hydrogen gas mixture over a solid while heating it at a linear rate. A detector downstream of the reactor is used to measure the change in hydrogen concentration as a function of temperature. Because the gas flow rate is constant, the change in hydrogen concentration is proportional to the rate of reduction. As stated by A. Jones (1986), TPR is widely used to evaluate catalyst preparation and regeneration techniques. The ease that a catalyst is reduced is important because they are activated by reduction. Information about the chemical composition and the concentration of the sample can be obtained from the position and area of the peaks.

3.7.1 TPR Experimental Procedure

Temperature programmed reduction experiments were done using an Autochem II 2920, as described in section 3.3.4.1. The catalyst samples were heated from 25 to 500°C at a heating rate of 10°C/min while passing 10% H_2/Ar (50 mL/min). During this time, the change in hydrogen uptake was quantified by associating the TCD signal with a calibration file and integrating the peaks using ORIGIN software.

3.7.2 TPO Experimental Procedure

Directly following temperature-programmed reduction, the samples were oxidized using an AutoChem II 2920. First, the samples were cooled from 500°C to 25°C at a

cooling rate of 10 K/min under a flow of helium (50 mL/min). The samples were then heated at a rate of 10°C/min to 500°C while passing 10% O_2/He (50 mL/min). Data for the change in gas composition as a function of temperature was collected at a sampling rate of 1 Hz. At the end of the analysis, the samples were cooled to 25°C while passing helium (50 mL/min).

3.8 Temperature Programmed Desorption (TPD)

Temperature programmed desorption of basic probe molecules (e.g. ammonia) is a common technique used to determine the acidity of solid catalysts. T. Bhaskar et al. (2001) states that ammonia is commonly used because of its stability, strong basic strength, and small size. According to J.L Falconer (1993) and T. Bhaskar et al. (2001), temperature programmed desorption is advantageous because of its reproducibility and its ability to measure low coverages that cannot be detected with adsorption experiments. However, J.L. Falconer (1993) acknowledges that readsorption and diffusion limitations of the analysis gas are some of the disadvantages involved with the technique. He explains that the flow rate of the carrier gas has a large influence on the accuracy of results, concluding that low flow rates contribute to increased diffusion limitations and readsorption while high flow rates reduce the concentration of desorbed species.

In a TPD experiment, the catalyst is exposed to an adsorbing gas until saturation of the surface occurs. After saturation, excess adsorbing gas is flushed away with an inert gas, the catalyst is heated at a linear rate under the inert gas, and the concentration of desorbed gases is monitored downstream of the catalyst. In most cases, a thermal conductivity detector is used to monitor the concentration of the gas.

In this study, NH_3 was used as the analysis gas to study the acidity of the catalyst surface. The desorption profile consisted of a series of peaks that corresponded to a specific type of adsorption site. Information regarding the strength and concentration of adsorption sites was obtained from the position and area of the peaks.

3.8.1 TPD Experimental Procedure

Temperature programmed desorption experiments were carried out in an AutoChem II 2920. Prior to TPD analysis, the samples were preteated by passing ultra-high pure helium over the catalyst while heating from 25°C to 200°C, pausing at 200°C for 60 minutes, and cooling to 80°C. After the samples were held at 80°C for 10 minutes, they were dosed with 14.9 % NH_3/He (15 mL/min) for 30 minutes. Excess ammonia was removed by passing ultra-high pure helium (25 mL/min) for 60 minutes. Desorption was carried out from 80°C to 500°C at a heating rate of 10°C/min. During this time, the thermal conductivity signal was recorded at a rate of 1 Hz. The same procedure, all the way from cooling to 80°C and heating to 500°C was repeated three more times with heating rates of 5, 15, and 20°C/min. The amount of NH_3 desorbed was quantified by integrating the peaks with ORIGIN software.

3.9 Ring Opening Reaction

Reaction studies were done at 300°C and atmospheric pressure with methyl-cyclopentane (mcp) as the probe molecule. Because of instrumental constraints, mcp was injected onto the catalysts, as apposed to it being continuously passed. The reaction products were identified by collecting mass to charge data as a function time, consisting

of peaks corresponding to the mcp injections, with a mass spectrometer. The disappearance of mcp was determined by comparing the peak areas for pure and reacted mcp.

3.9.1 Ring Opening Reaction Procedure

The reaction studies were carried out using an AutoChem II 2920 and a mass spectrometer. The samples were prepared for analysis according to Section 3.5.2. Sample pretreatment was done using temperature programmed reduction, as outlined in Section 3.6.1, and cooling to 300°C in 10% H_2/Ar (10 mL/min). After pre-treatment of the samples, they were dosed with eight 0.13 mL injections of mcp at atmospheric pressure. Methyl-cyclopentane vapor was generated by filling a threaded 50 mL Erlenmeyer flask with mcp, placing the flask into the vapor generator heating mantle, immersing the aerator into the flask, and screwing it into the vapor generator port located under the front panel of the Autochem II 2920. The mcp was vaporized by setting the temperature of the flask and reflux to 50 and 45°C, creating a mcp partial pressure of 41 kPa, and carried to the loop by passing 10% H_2/Ar (10 mL/min). Injecting the contents of the loop was done by switching the loop valve from fill to inject, injecting the contents of the loop onto the sample, allowing 10 minutes for the vapor to flow over the sample, switching the loop valve back to fill, and refilling the loop with vapor for 5 minutes until the next dose was injected.

3.9.2 Dycor Quadrupole Gas Analyzer

A Dycor quadrupole gas analyzer from Ametek was used to analyze the reaction products by leaking the analysis gas from the AutoChem II 2920 into its vacuum chamber. A Leybold trivac D1 6B roughing pump and a TPU 060 turbomolecular pump were used to achieve a pressure of 1 x 10^{-6} Torr inside the chamber. The mass spectrometer was operated in bar mode and mass to charge ratios from 1 to 84 were scanned. When gas molecules in the inonizer region of the Analyzer Head were bombarded with electrons that were emitted from the hot filament, ions of the parent molecules and ion fragments were produced (*Dycor Quadrupole Gas Analyzer Operating Instructions for models: M100, MA100, M200, MA200, M100M, MA10M, M200M, MA200M*, 1994). The ions were sent towards the mass filter by electric fields produced by the focus electrode. At the mass filter, ions with certain mass to charge ratios were permitted to pass. These ions were converted to an electric current that was proportional to their partial pressure. The signals were converted to digital signals and transferred from the control unit to the PC with a RS-232 cable.

CHAPTER: 4 RESULTS

4.1 Elemental Compositional Analysis (XPS)

Each catalyst was prepared by calculating the amount of precursor required through a mole balance. XPS was used to verify the final Mo/Zr atomic ratio. The experimental Mo loading was determined from the XPS spectra by assuming that Zr and Mo existed as ZrO_2 and MoO_3, integrating the peaks positioned at the O (1s), Zr (3d), and Mo (3d) binding energies, and normalizing the peak areas with a relative sensitivity factor. The Mo/Zr and O/(Mo + Zr) atomic ratios were calculated by dividing the atomic concentration of zirconium by molybdenum and dividing the atomic concentration of oxygen by molybdenum plus zirconium. The theoretical amount of oxygen was calculated by assuming that oxygen was present as ZrO_2 and MoO_3. The results are shown in Table 4-1.

Table 4-1
Predicted and experimental XPS data

Atomic Ratio[a] (Mo/Zr)	Atomic Ratio[b] (Mo/Zr)	Atomic Ratio[c] (O/(Mo+Zr))	Atomic Ratio[b] (O/(Mo+Zr))	Peak	Position BE (eV)	Raw Area ($CPSx10^5$)	RSF	Atomic Conc. (±1%)
0	0	2	2.18	O 1s	529	9.4	0.78	45.7
				C 1s	283	2.4	0.28	33.4
				Zr 3d	181	13.7	2.58	20.9
				Mo 3d	236	0	3.32	0
0.02	0.03	2.03	2.26	O 1s	528	13.0	0.78	47.8
				C 1s	283	2.9	0.28	31.1
				Zr 3d	180	17.6	2.58	20.5
				Mo 3d	231	7.5	3.32	0.7
0.05	0.05	2.05	2.36	O 1s	528	13.1	0.78	47.1
				C 1s	283	3.2	0.28	32.9
				Zr 3d	181	16.7	2.58	19.0
				Mo 3d	231	1.1	3.32	0.9
0.07	0.09	2.09	2.40	O 1s	528	13.0	0.78	48.0
				C 1s	283	3.0	0.28	32.1
				Zr 3d	181	15.7	2.58	18.3
				Mo 3d	231	1.9	3.32	1.7
0.10	0.11	2.11	2.41	O 1s	529	11.8	0.78	48.2
				C 1s	283	2.7	0.28	31.8
				Zr 3d	181	13.9	2.58	17.9
				Mo 3d	231	2.2	3.32	2.2
0.15	0.16	2.16	2.50	O 1s	529	11.8	0.78	49.2
				C 1s	283	2.6	0.28	31.1
				Zr 3d	181	12.6	2.58	16.6
				Mo 3d	231	3.1	3.32	3.1
0.20	0.19	2.19	2.37	O 1s	529	12.7	0.78	50.9
				C 1s	283	2.8	0.28	27.6
				Zr 3d	181	13.7	2.58	17.5
				Mo 3d	231	4.1	3.32	4.0

[a]Atomic ratios from mole balance calculations [b]Atomic ratios obtained from XPS data. [c]Atomic ratios if no other forms but ZrO_2 and MoO_3 exist.

As can be seen in Table 4-1, the predicted and experimental Mo/Zr atomic ratios were in excellent agreement. The predicted and experimental Mo/Zr atomic ratios differed by a maximum of 8 % for catalysts containing 0 at. %, 5 at. %, 11 at. %, 16 at. % and 19 at. % molybdenum. Catalysts containing 3 at. % and 9 at. % molybdenum differed by 58 % and 24 %, respectively. The slight discrepancy between the predicted and experimental values was explained by the precision with which the catalyst precursors were weighed. Although an analytical balance accurate to 0.0001 g was used to weigh the precursors, it was difficult to weigh the exact amount of required precursor.

The predicted O/(Mo+Zr) atomic ratios were all lower than the experimental O/(Mo+Zr) atomic ratios. Additional oxygen was likely present as CO, CO_2, or OH, or as another Mo-O phase. The maximum difference between the predicted and experimental O/(Mo+Zr) was 16 % for 16 at. % molybdenum.

In addition to the XPS data for O (1s), Zr (3d), and Mo (3d), the XPS data for C (1s) was also reported in Table 4-1. The presence of C (1s) was a result of atmospheric contamination and did not significantly change between catalysts.

4.2 Crystalline Structure (XRD)

X-ray diffraction was used to determine the crystalline structure and lattice parameters of the catalysts. Figure 4-1 shows the XRD patterns for all of the catalysts. Dashed vertical lines superimposed on the XRD patterns represent a standard cubic reference pattern (JCPDS file no. 27-997) (Bhattacharyya et al., 2001). As can be seen by the lines, the crystalline structure appeared to be cubic for catalysts containing 9 to 16 at. % molybdenum. Catalysts containing less than 9 at. % molybdenum had peaks at

$2\theta = 28^{\circ}$ and $2\theta = 32^{\circ}$ that decreased with molybdenum loading, indicating a gradual phase transition from monoclinic to cubic (Calafat et al., 2000). Schematic diagrams showing the monoclinic, cubic, and tetragonal crystalline structures are shown in Figure 4-2.

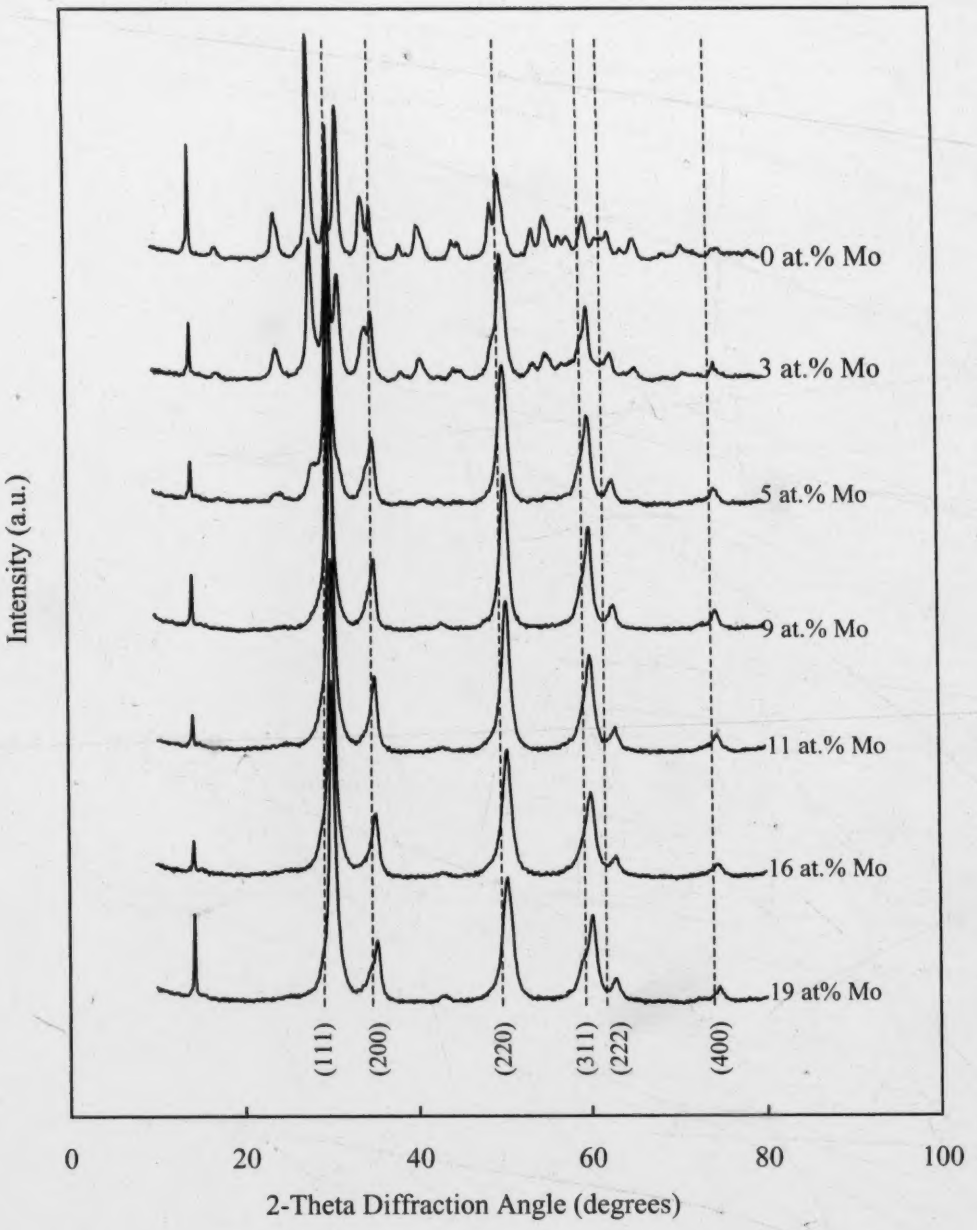

Figure 4-1: XRD pattern of molybdenum-zirconium oxides. The dotted lines represent a standard cubic reference pattern (JCPDS file no. 27-997) for cubic ZrO_2.

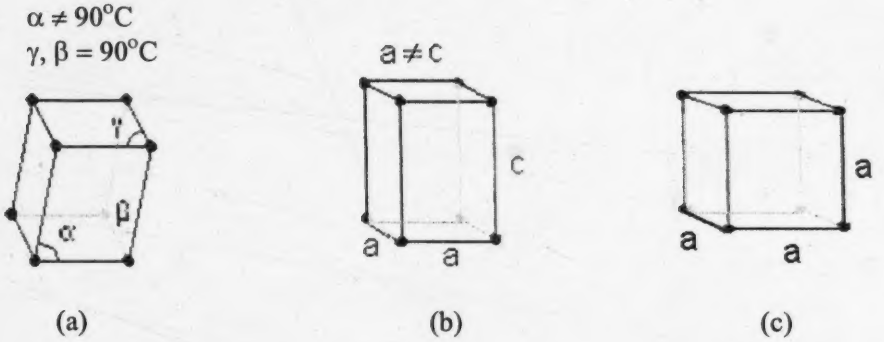

Figure 4-2: Monoclinic (a), tetragonal (b), and cubic (c) crystalline structures.

Many studies have shown that pure ZrO_2 exists primarily in the monoclinic phase and incorporation of molybdenum promotes a phase transition to the tetragonal phase. Calafat et al. (2000) reported that ZrO_2-MoO_3 catalysts containing 0.1 at. % to 0.5 at. % molybdenum were in the tetragonal phase whereas pure zirconia was primarily in the monoclinic phase. Another study conducted by Zhao et al. (1997) showed that MoO_3-ZrO_2 catalysts containing 14 at. % molybdenum were in the tetragonal phase. The main difference between cubic and tetragonal XRD patterns, as stated by Hamon et al. (1991), was the presence of 2 double peaks and 2 single peaks at $2\theta=35^\circ$ and $2\theta=60^\circ$ for tetragonal and cubic structures. However, cubic and tetragonal zirconia were not distinguished in the present study.

Calafat et al. (2000) speculated the formation of a new Mo-Zr phase for catalysts prepared by co-precipitation, having a Mo/Zr ratio of 0.5 and calcination temperature of 700°C. The XRD patterns for these catalysts were consistent with the JCPDS Powder Diffraction File for $Zr(MoO_4)_2$. In the present study, the XRD pattern for 19 at. %

molybdenum showed peak broadening at $2\theta=60^{o}$, indicating the formation of a new Mo-Zr phase.

The lattice parameters shown in Table 4-2 were calculated using Equations (3-2) and (3-3). For each catalyst, an average of the lattice parameters for the (111), (200), (220), (311), (222), and (400) was taken. The error was determined by calculating a 95 % confidence interval on the lattice parameters at each Mo/Zr ratio.

Table 4-2
X-Ray Diffraction Lattice Parameters

Atomic Ratio (Mo/Zr)	Cubic Lattice Parameter (Å)
0.09	5.10 ± 0.02
0.11	5.10 ± 0.01
0.16	5.10 ± 0.02
0.19	5.10 ± 0.02

4.3 CO_2 Adsorption (DSC)

The heat of CO_2 adsorption as a function of temperature for MoO_3-ZrO_2 catalysts is shown in Figure 4-3. Each point in Figure 4-3 was obtained by repeating the experiment three times and averaging the results. The error bars was determined by repeating each experiment at least three times and calculating the 95 % confidence interval.

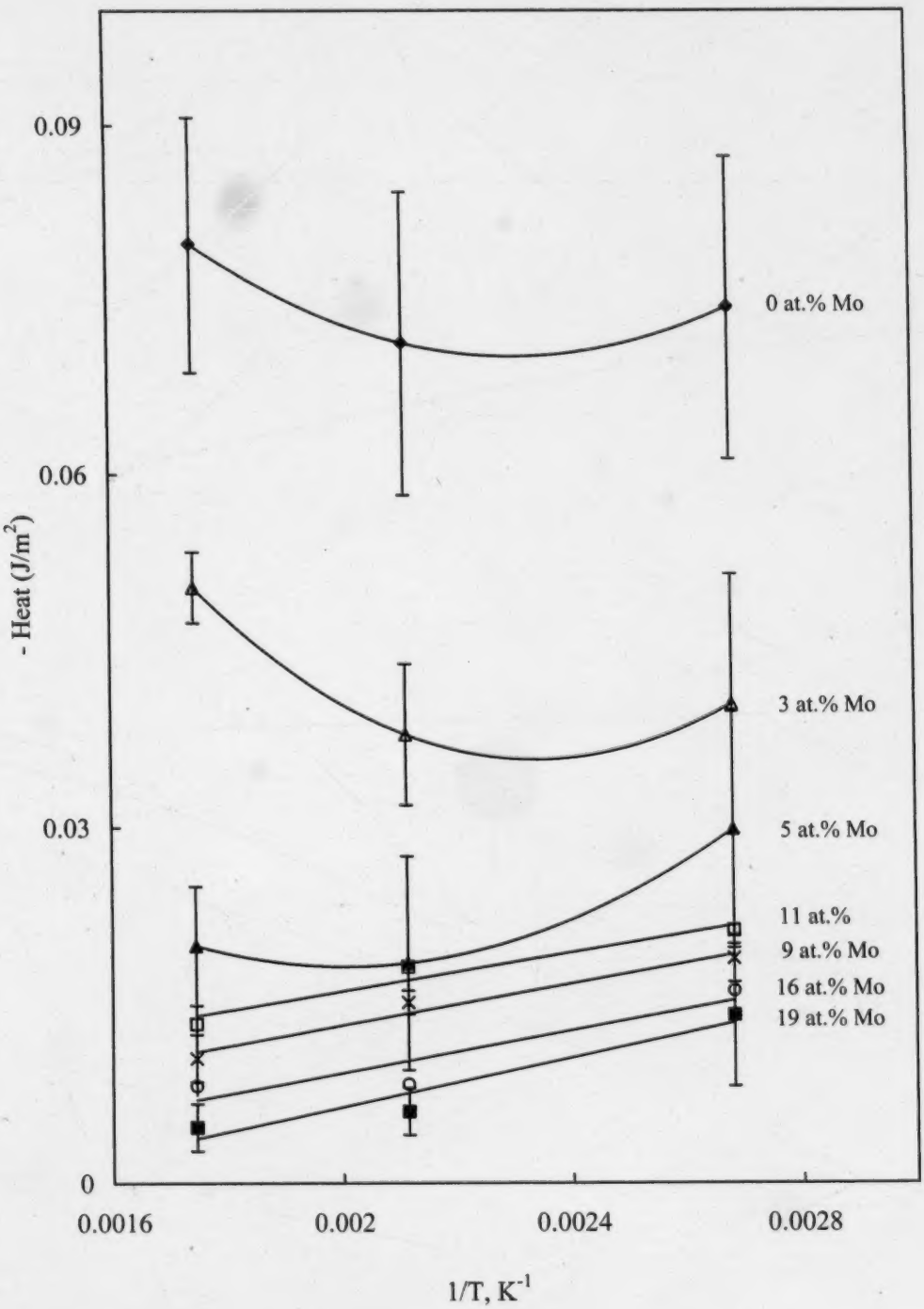

Figure 4-3: CO_2 adsorption of MoO_3-ZrO_2 catalysts.

As would be expected for an exothermic process, the heat of adsorption increased with decreasing temperature for catalysts having a cubic structure (Mo/Zr = 19 at.% to 11 at. %). For catalysts having a monoclinic cubic structure (Mo/Zr = 5 at. % to 0 at. %), the trend was gradually reversed. At 5 at. % molybdenum, the minimum heat of adsorption occurred at 200°C rather than at 300°C. At 3 at. % and 0 at. % molybdenum, the maximum heat of adsorption occurred at 300°C instead of 100°C.

For catalysts with a monoclinic crystalline structure, the heat of adsorption significantly decreased with increasing molybdenum concentration. Increasing the molybdenum concentration from 0 at % to 5 at. % caused the heat of adsorption to decrease by 0.04 ± 0.01 J/m^2 at 100°C For catalysts with cubic structures and molybdenum loadings from 11 at. % to 19 at. %., the heat of adsorption decreased by 0.01 ± 0.004 J/m^2 at 100°C.

As outlined in Section 3.4.3, the same sample was used to repeat the experiments. In each case, the heat of adsorption decreased as the experiment was repeated, indicating the presence of irreversible adsorption. The heats of adsorption for the first and last experiments are shown in Table 4-3. The maximum and minimum difference occurred at 5 at. % and 11 at. % molybdenum, respectively. The overall amount of irreversible adsorption decreased as the temperature increased from 100°C to 300°C.

Table 4-3
Heat of adsorption of the first and third experiment of MoO_3/ZrO_2 catalysts

Atomic Ratio (Mo/Zr)	First Heat of CO_2 Adsorption ($\times 10^{-2} \pm 1 \times 10^{-2}$ J/m^2) Temperature (°C)			Last Heat of CO_2 Adsorption ($\times 10^{-2} \pm 1 \times 10^{-2}$ J/m^2) Temperature (°C)		
	100	200	300	100	200	300
0	7.9	7.7	8.3	6.9	6.8	8.1
0.03	5.3	4.4	5.4	4.2	3.4	4.8
0.05	3.5	2.3	2.3	2.7	1.7	1.9
0.09	3.6	1.9	1.4	2.8	1.3	1.0
0.11	1.8	1.1	1.1	1.7	1.3	0.9
0.16	2.0	1.3	0.9	1.4	0.6	0.6
0.19	1.8	0.7	0.5	1.4	0.5	0.4

4.4 BET Surface Area

Table 4-4 shows the effect of molybdenum loading on BET surface area of the MoO_3-ZrO_2 catalysts. The BET surface area values for the present study were obtained by taking an average of two experiments. The maximum difference between successive experiments was 2.6 %. The error was calculated by repeating the surface area measurement of 11 at. % molybdenum 10 times and calculating the 95% confidence interval.

The surface area increased with molybdenum loading for catalysts containing 0 at. % to 16 at. % molybdenum and then decreased. A comparison between BET surface areas previously reported in the literature for catalysts prepared using different techniques is shown in Table 4-5. With increasing molybdenum concentration, the BET surface area increased to a maximum value (S_{max}) and then decreased for catalysts prepared by co-precipitation or hydrogel impregnation. Catalysts prepared by hydrogel impregnation gave catalysts with larger S_{max} values compared to catalysts prepared by co-precipitation.

Catalysts prepared by incipient impregnation gave catalysts with significantly lower surface areas that decreased with molybdenum content.

Table 4-4
Effect of the Mo/Zr ratio on the BET surface area

Atomic Ratio (Mo/Zr)	BET Surface Area ($\pm$ 0.9 m^2/g)
0	20
0.03	31
0.05	63
0.09	78
0.11	101
0.16	124
0.19	111

Table 4-5
BET surface area for different methods of MoO_3-ZrO_2 preparation techniques.

Atomic Ratio (Mo/Zr)	BET Surface Area (m^2/g)
0	20 ± 0.9^a, 42^b, 96^f,52^g, 84^h
0.01	43^h
0.02	37^h
0.03	31 ± 0.9^a, 131^f,87^g, 27^h
0.05	63 ± 0.9^a, 26^h
0.06	23^h
0.08	13^h, 156^f,140^g
0.09	78 ± 0.9^a, 36^e
0.10	100^b, 125^b
0.11	101 ± 0.9^a
0.14	218^f,186^g
0.16	124 ± 0.9^a
0.19	111 ± 0.9^a
0.20	116^b, 139^c, 37.6^d
0.22	307^f,224^g
0.23	43^e
0.27	310^f,210^g
0.29	34.0^d
0.30	84^b, 137^b
0.36	304^f,159^g
0.38	33.0^d
0.44	255^f,144^g
0.50	69^b, 140^c

[a]From this study. [b]From Calafat et al. (2000), prepared by co-precipitation and calcined at 773 K for 2 h. [c]From Calafat et al. (2000); prepared by the sol-gel method and calcined at 773 K for 2 h. [d]From Maity et al. (2000); prepared by incipient impregnation and calcined at 723 K for 6 h. [e]From Li et al. (1997); prepared by incipient impregnation and calcined at 1073 K for 3 h. [f]From Zhao et al. (1997); prepared by hydrogel impregnation and calcined at 723 K. [g]From Zhao et al. (1997); prepared by hydrogel impregnation and calcined at 823 K. [h]From Bhaskar et al. (2001), prepared by incipient wetting of ZrO_2 and calcined at 500°C for 6h.

Calafat et al. (2000) conducted a study that employed co-precipitation and gave comparable surface area results to those obtained in this study for molybdenum loadings of 10 to 20 at %. Surface areas obtained by Calafat et al. (2000) for molybdenum loadings of 10 and 20 at. % were 100 and 116 m^2/g. In the present study, surface area values of 101 and 111 m^2/g were observed for catalysts containing 11 and 19 at. % molybdenum. Catalysts containing the same molybdenum loadings were not available for comparison between the two studies, possibly resulting in the difference of S_{max}. In the present and previous studies, S_{max} was 124 m^2/g at 16 at. % molybdenum and 116 m^2/g at 20 at. % molybdenum.

The BET surface area of pure zirconia in the present study was at least 22 m^2/g lower than the values reported in other studies. In previous studies, values of 52, 42, 96 and 43 m^2/g were reported for calcination temperatures of 550, 500, 450, and 450°C. Zhao et al. (1997) showed that lowering the calcination temperature gave higher surface areas. However, when the above values were compared, the calcination temperature did not seem to have a systematic effect on surface area.

4.5 Temperature Programmed Reduction (TPR)

Figure 4-4 shows the TPR spectra of the MoO_3-ZrO_2 catalysts. No peaks were present in the spectra for 0 at. % molybdenum, showing that pure ZrO_2 is not reducible up to 500°C. Catalysts containing 3 at. % molybdenum showed a one-peak spectrum that transformed to a two-peak spectrum at 5 at. % molybdenum. With further molybdenum loading, the two peaks became more pronounced, suggesting that reduction occurred in two stages.

The total area under each curve or hydrogen uptake increased with molybdenum loading, indicating that the catalysts were more reducible at higher molybdenum loadings. The position of the peaks also shifted to a lower temperature with increasing molybdenum loading, showing that the catalysts were more easily reduced. The total area under each curve was found using the trapezoidal rule. A Gaussian peak fitting function in ORIGIN was used to fit two peaks to every spectrum, with the exception of the spectra for 0 at. % and 3 at. % molybdenum. The error in total hydrogen uptake was calculated by obtaining 6 TPR measurements for the catalyst containing 5 at. % molybdenum and calculating a 95 % confidence interval.

Table 4-6 shows the effect of Mo/Zr atomic ratio on the total hydrogen uptake, the hydrogen uptake at each peak, and the peak temperature per surface area and per mass of catalyst. The experiments were repeated twice and an average value was reported. The summation of the hydrogen uptake for Mo-O and Zr-O was less than the total hydrogen uptake for each catalyst. Consistent with the appearance of the raw spectra, the calculated hydrogen uptake increased and temperature of the peaks decreased with molybdenum loading.

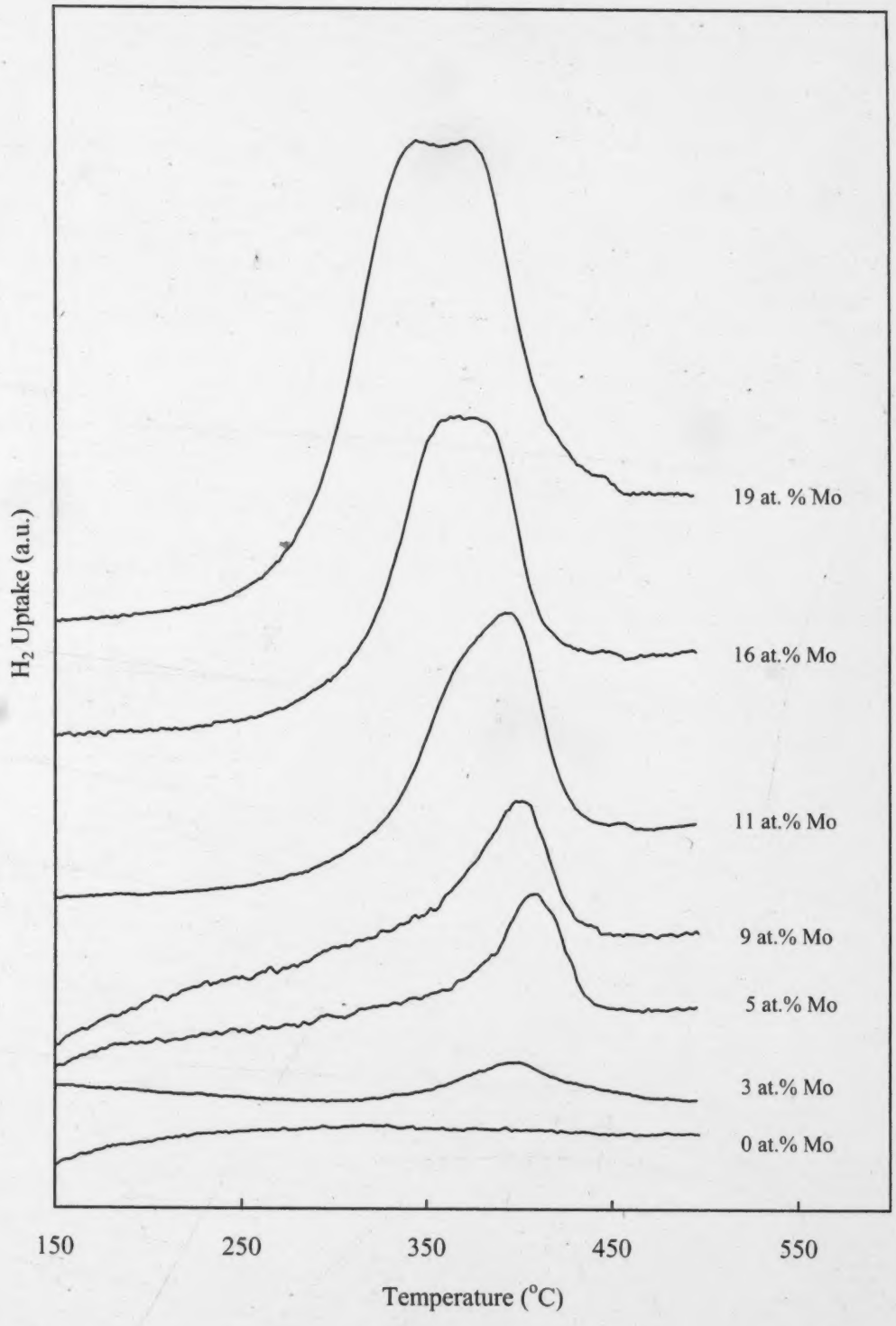

Figure 4-4: TPR profiles of MoO_3-ZrO_2 catalysts.

Table 4-6
Effect of Mo/Zr atomic ratio on H_2 uptake per g_{cat}

Atomic Ratio (Mo/Zr)	H_2 Uptake (x 10^{-2}mL/m^2_{cat})			H_2 Uptake (mL/g_{cat})			Peak Temperature (°C)	
	Mo-O (±0.1)	Zr-O (±0.7)	Total (±1.2)	Mo-O (±0.1)	Zr-O (±0.4)	Total (±0.8)	Mo-O (±18)	Zr-O (±10)
0								
0.03			4.8			1.5		
0.05	1.3	2.6	5.9	0.6	2.5	2.9	365	407
0.09	2.0	4.3	8.0	1.6	3.3	6.2	365	402
0.11	2.6	4.3	7.4	2.6	4.3	7.5	357	395
0.16	3.9	3.8	9.1	4.8	4.7	11.3	350	385
0.19	6.7	6.8	15.0	7.5	7.6	16.7	333	379

To further illustrate the effect of molybdenum loading on the total hydrogen uptake per surface area of catalyst, the hydrogen uptake as a function of molybdenum loading is shown in Figure 4-5. Overall, the hydrogen uptake increased with molybdenum loading, but the rate of increase depended on the crystalline structure of the catalysts. Two distinct trend lines corresponding to two different crystalline regions were fit to the data. The increase of hydrogen uptake with molybdenum loading was much greater in the monoclinic region than in the cubic region. The catalyst containing 19 at. % molybdenum did not fit the trend line that was drawn for the cubic catalysts, indicating that its crystalline structure was not entirely cubic.

Figure 4-6 shows the total hydrogen uptake per gram of catalyst as a function of molybdenum loading. The hydrogen uptake increased linearly with molybdenum loading and the effect of crystallinity was not apparent. Comparing Figure 4-5 and 4-6 shows that the crystalline structure had an effect on the hydrogen uptake.

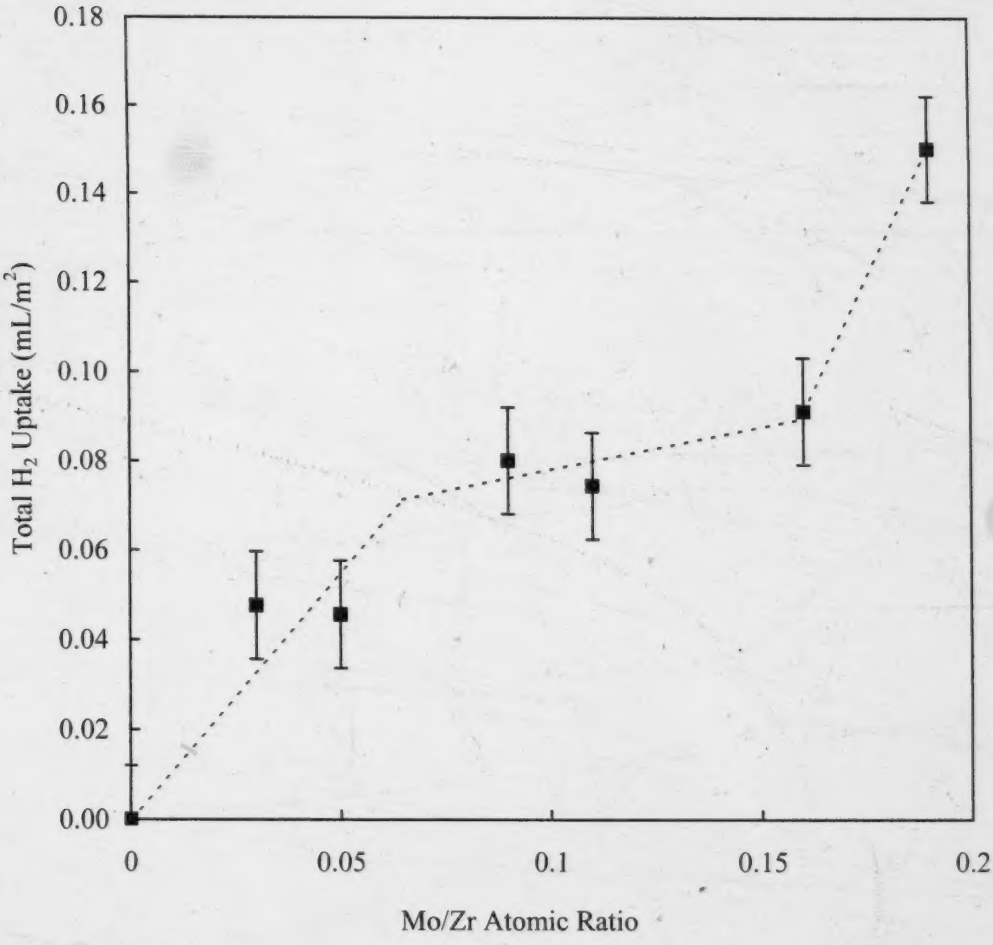

Figure 4-5: Variation of total hydrogen uptake with Mo-loading, per m^2_{cat}.

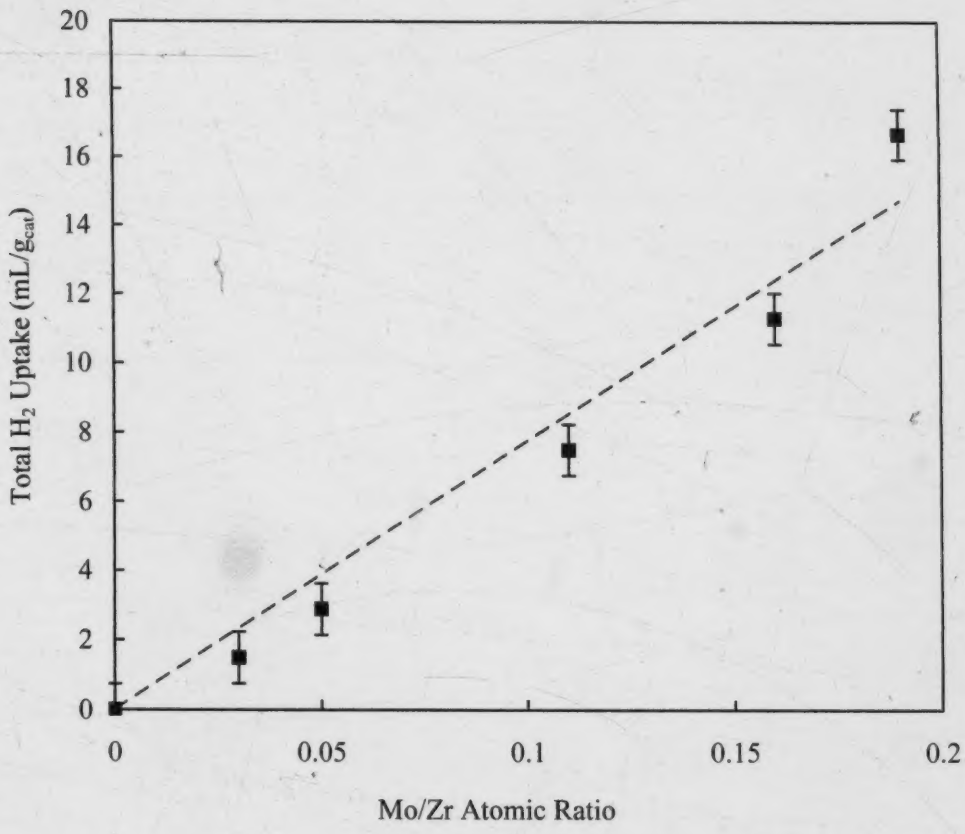

Figure 4-6: Variation of total hydrogen uptake with Mo-loading, per g_{cat}.

4.6 Temperature Programmed Oxidation (TPO)

TPO profiles of MoO_3-ZrO_2 catalysts are presented in Figure 4-7. Consistent with the temperature programmed reduction spectra, the total area under each curve or oxygen uptake increased with molybdenum loading. The increase in oxygen uptake with molybdenum loading suggested that the catalysts were returned to their unreduced state. Table 4-7 shows the total hydrogen uptake, the hydrogen uptake at each peak, and the peak temperature per surface area of catalyst prior to and following TPO for catalysts containing 11 at. % and 19 at. % molybdenum. The pre and post-TPO values agreed within error, suggesting that the catalysts were returned to their unreduced state after treatment with TPO.

Table 4-7 TPR results prior to and following treatment with TPO.

Mo/Zr (at. %)	H_2 Uptake (x 10^{-2}mL/m^2_{cat})			H_2 Uptake (mL/g_{cat})			Peak Temperature (°C)	
	Mo-O (±0.1)	Zr-O (±0.7)	Total (±1.2)	Mo-O (±0.1)	Zr-O (±0.4)	Total (±0.8)	Mo-O (±18)	Zr-O (±10)
11[1]	2.6	4.3	7.5	2.6	4.3	7.6	357	395
11[2]	2.3	4.3	7.3	2.3	4.3	7.4	385	387
19[1]	6.7	6.8	15.3	7.5	7.6	16.9	333	379
19[2]	7.0	7.0	14.8	8.0	8.0	16.4	340	385

[1]Pre-TPO. [2]Post-TPO.

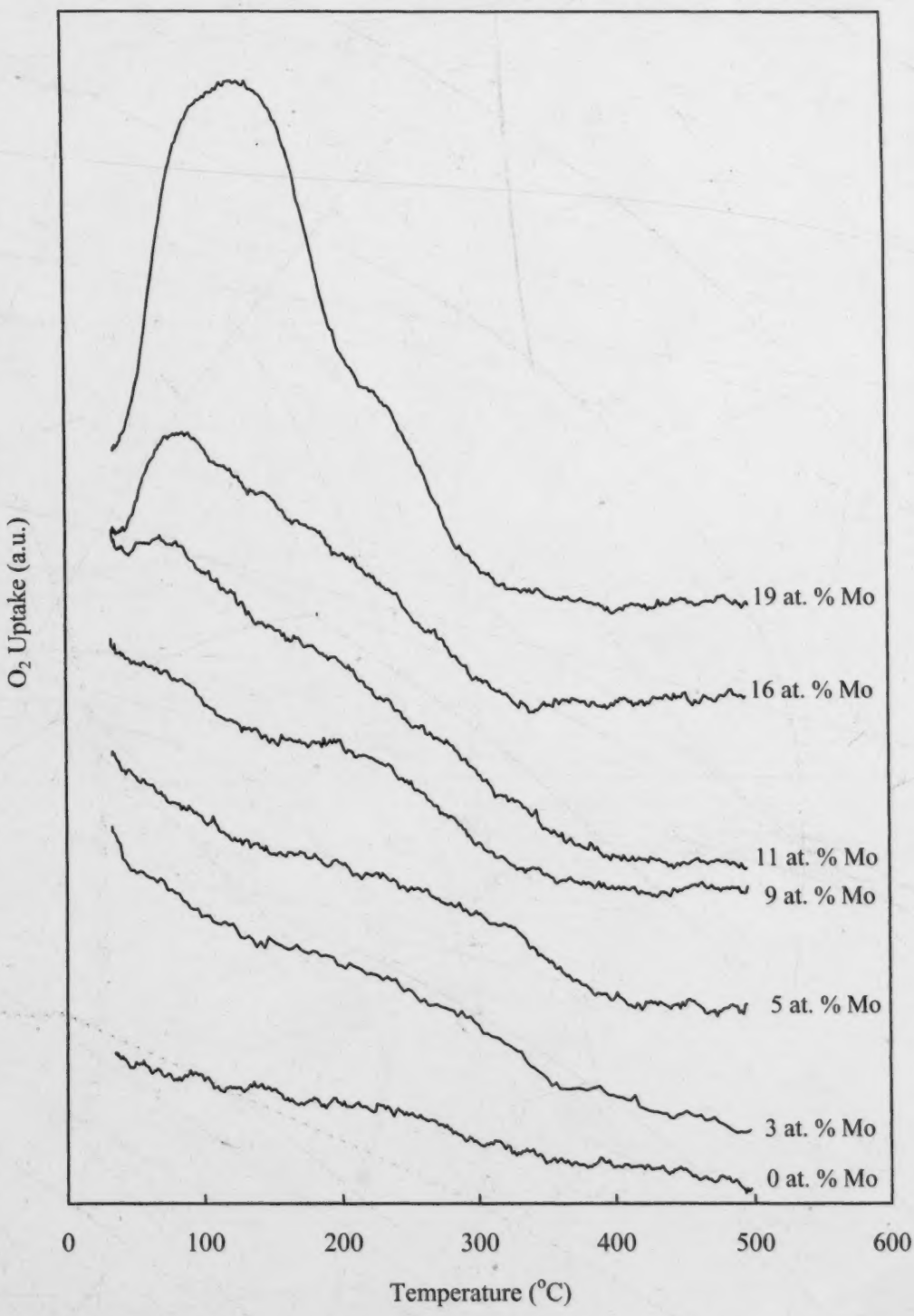

Figure 4-7: TPO profiles of MoO_3-ZrO_2 catalysts.

4.7 Temperature Programmed Desorption (TPD)

Ammonia (NH_3) temperature programmed desorption profiles of MoO_3-ZrO_2 catalysts, for constant catalyst mass, are presented in Figure 4-8. Each spectrum consisted of two NH_3 desorption peaks, corresponding to strong and moderate acidic sites. Irrespective of molybdenum loading, the first and second peak occurred at around 150 and 300°C. With increasing molybdenum loading, the peak intensity, or amount of acid sites, increased.

The peak area corresponding to the volume of desorbed ammonia was numerically integrated using the trapezoidal rule. Although the data suggested the presence of two peaks, two peaks were not resolved because of their broadness. The error in the volume of desorbed ammonia was determined by calculating the 95 % confidence interval using 3 data points for a catalyst containing 11 at. % molybdenum.

The volume of ammonia desorbed per unit mass and per unit surface area are shown in Figures 4-9 and 4-10. Figure 4-9 shows that the acid site concentration linearly increased as the molybdenum loading increased. A break in the data occurred at 5 at. % molybdenum loading, at the same concentration where a phase shift from monoclinic to cubic, occurred. In the cubic region, the rate of increase of volume desorbed with molybdenum loading was slightly faster.

Figure 4-10 shows that the desorbed volume per unit surface area decreased with molybdenum loading. The data was fit to a second order polynomial with a minimum desorption volume at 11 at. % molybdenum. From 0 to 5 at. % molybdenum loading, the catalyst was in the monoclinic phase and exhibited a rapid decrease in desorbed volume as the molybdenum loading increased. Catalysts in the cubic phase containing 11 to 16

at. % molybdenum had approximately the same desorbed volumes. At 19 at. % molybdenum, the desorbed volume was approximately the same as for 5 at.% molybdenum.

4.3.8 Ring-Opening Reaction

Reaction data for methyl-cyclopentane is shown in Table 4-8. The conversion of mcp was monitored by integrating the peaks of m/z = 41, 56, and 69 as a function of time, which corresponded to injections of mcp. Mass-to-charge ratios of 41, 56, and 69 were monitored because they are the most abundant for mcp, having relative abundances of 494, 999, and 353. Any m/z ratios for mcp with lower relative abundances did not have spectra with discernable peaks. Reaction data are only presented for a m/z ratio of 56 because the data for m/z ratios of 41 and 69 was inconsistent, even though the peaks were discernible.

Each peak area shown in Table 4-8 is an average of at least 2 injections. All of the catalysts were injected with eight doses of mcp, but 8 peaks did not show up in every spectrum, possibly due to insufficient filling time of the loop. For spectra that contained eight peaks, the peak areas did not systematically increase or decrease with injection. The error was calculated by injecting mcp into an empty tube 8 times and calculating the 95 % confidence interval on the peak areas.

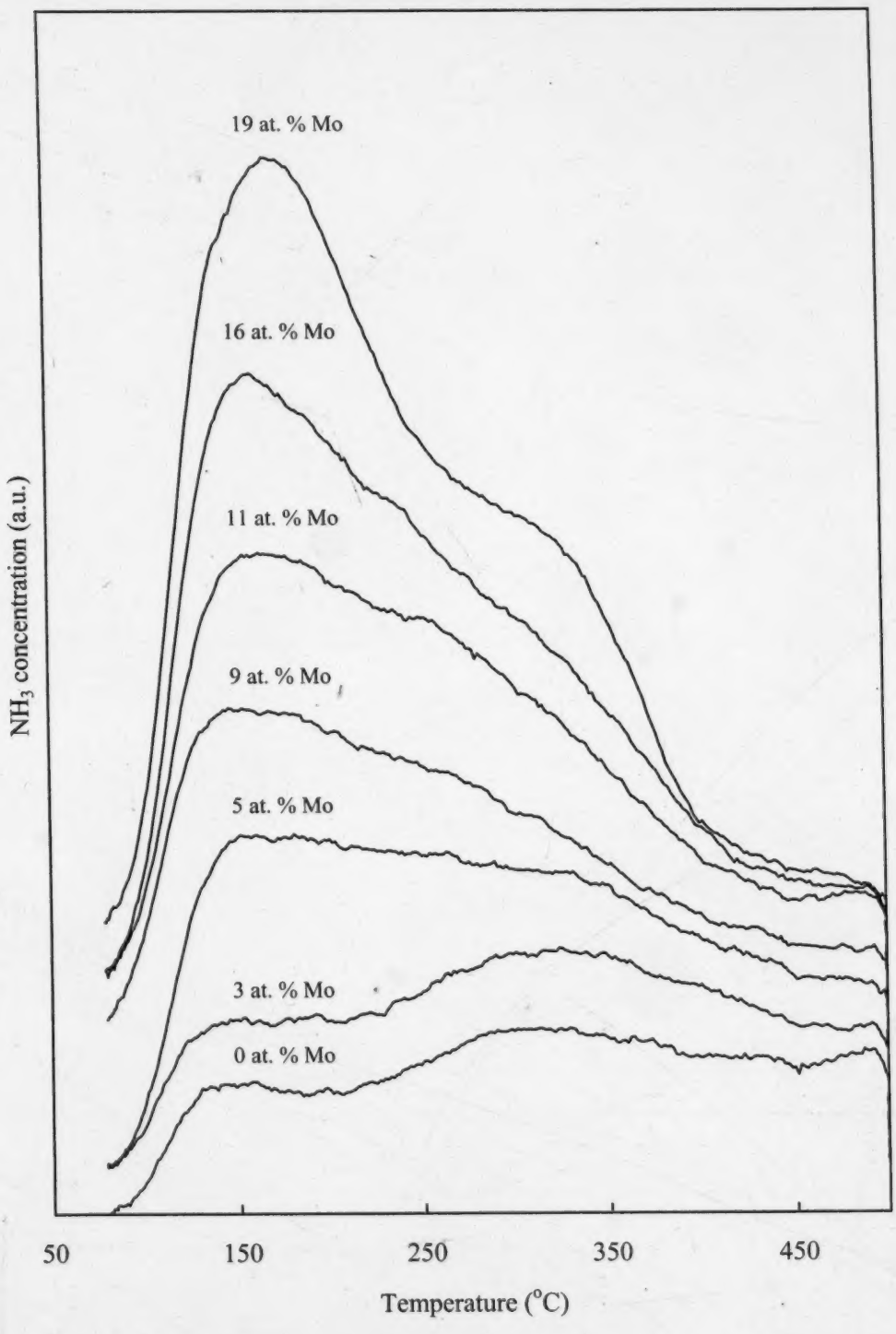

Figure 4-8: Ammonia TPD profiles of MoO_3-ZrO_2 catalysts.

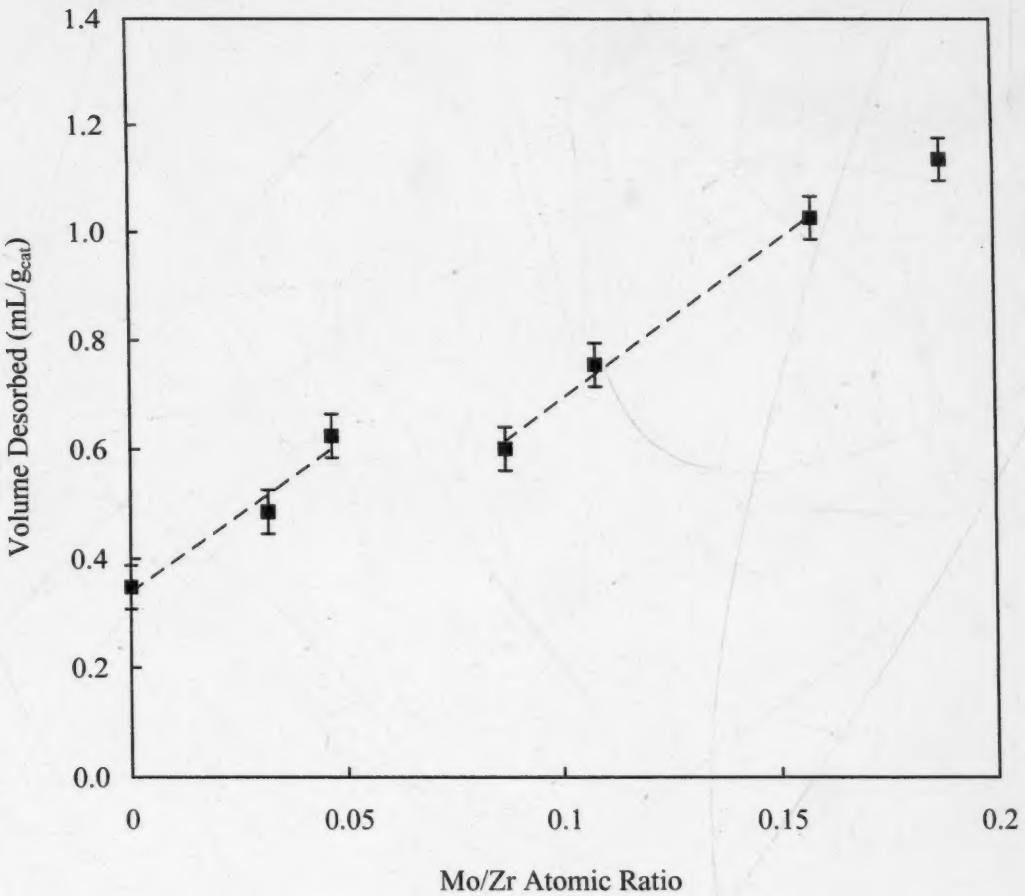

Figure 4-9: Volume of NH_3 desorbed per unit mass of MoO_3-ZrO_2 catalysts.

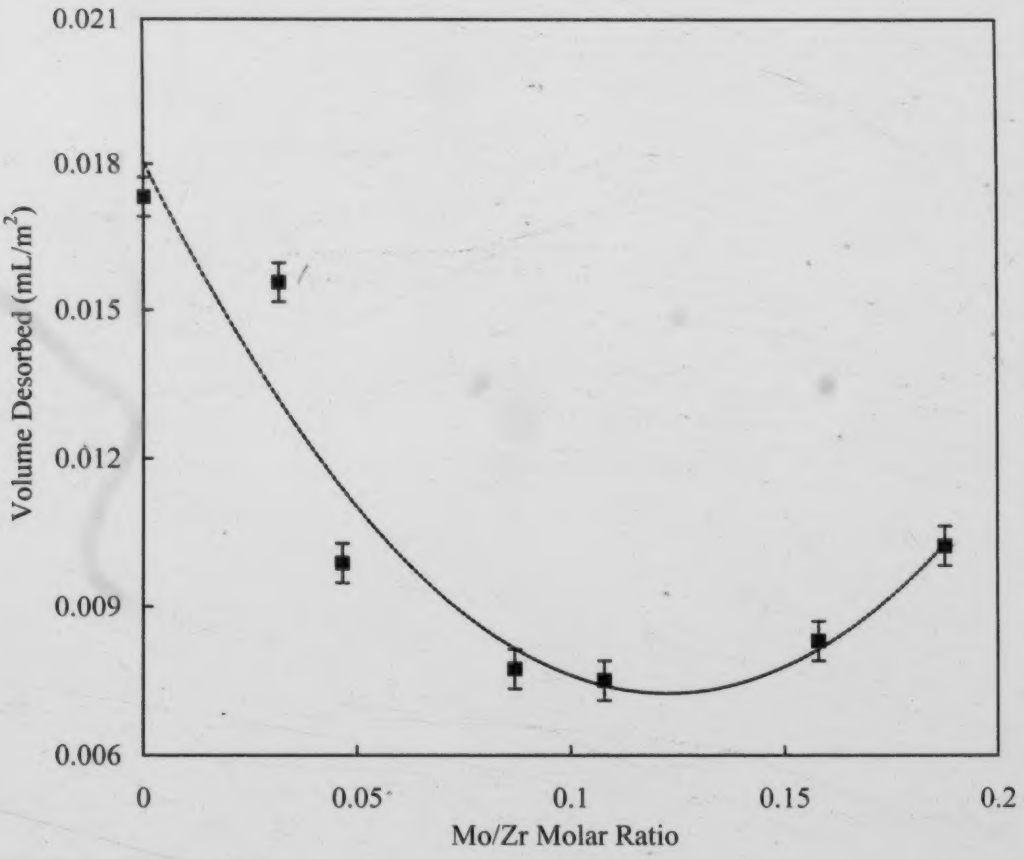

Figure 4-10: Volume of NH_3 desorbed per unit surface area of MoO_3-ZrO_2 catalysts.

Table 4-8
Conversion of methyl-cylcopentane based on data for m/z = 56.

Atomic Ratio (Mo/Zr)	Peak Area (x 10^{-6} ± 0.2 x 10^{-6} a.u.)	Conversion (%)
Blank 1	**3.3**	
0	3.0	9.1
0.03	2.1	36.4
0.09	3.2	3.0
0.19	3.0	9.1
Blank 2	**4.3**	
0.05	5.0	N/A
0.11	4.1	4
0.16	4.3	N/A

The peak areas for pure mcp were denoted as blank 1 and blank 2. Blank runs were carried under the same conditions as for the reactioins. Calibration of vapors is possible using the Autochem II 2920. An attempt was made to calibrate the instrument for reflux temperatures of 35, 45, and 55°C to directly monitor the disappearance of mcp with the TCD signal. However, after running an empty sample tube under the conditions for calibration (tube temperature = 24°C), it was found that the TCD signal depended on the tube temperature. Because of the built in calibration function, the tube temperature could not be set during calibration.

The first four results in Table 4-8 can be compared to blank 1 and the last three results can be compared to blank 2. The peak areas were within 9 % of their respective blanks, excluding 0.03 and 0.05 Mo/Zr.

All of the m/z ratios, from 1 to 84, were more closely examined for 19 at. % molybdenum. Peaks were observed in the data for m/z ratios of 1, 3, 20, and 40. The peaks for m/z ratios of 20 and 40 had relative abundances that were approximately 100

times higher than the relative abundance of the m/z ratios of mcp. These peaks were assigned to the argon, which was present as a carrier gas. No peaks were observed for hydrogen at a m/z ratio of 2.

CHAPTER 5: DISCUSSION

5.1 Elemental Compositional Analysis (XPS)

XPS is widely used for determining the surface composition and oxidation state of solids. The technique is extremely reliable and gives results that are accurate to 1%. The objective of using XPS in this study was to verify the elemental composition of the catalysts. The Mo/Zr atomic ratios that were determined from the XPS results were compared to the expected Mo/Zr atomic ratios that were calculated from the mole balances. The experimental Mo loading was determined from the XPS spectra by assuming Zr and Mo existed as ZrO_2 and MoO_3. This assumption was validated with the X-ray diffraction patterns.

Catalysts containing 5, 11, 16, and 19 at. % molybdenum had experimental Mo/Zr atomic ratios that were within 8 % of the predicted values. The catalyst precursors were carefully weighed using an analytical balance accurate to 0.0001 g, but weighing to this accuracy was difficult. The most difficultly with weighing the exact amount of precursor was encountered with the catalyst requiring the least amount of molybdenum (0.445 g). The error between the predicted and experimental Mo/Zr atomic ratio for this catalyst (Mo/Zr = 0.03) was 58 %.

Incomplete dissolution of the catalyst precursors prior to precipitation may have been another source of error. The precursors were heated in an aqueous solution to ensure that they were completely dissolved, but due to the limitations of the human eye, some particles may not have dissolved. If all of the particles were not dissolved, surface heterogeneities may have resulted and may not have been detected by XPS.

The theoretical amount of oxygen was calculated by assuming that oxygen was present as ZrO_2 and MoO_3. The predicted O/(Mo+Zr) atomic ratios were all lower than the experimental O/(Mo+Zr) atomic ratios. Additional oxygen was likely present as CO, CO_2, OH, or as another Mo-O phase. The maximum difference between the predicted and experimental O/Mo+Zr was 16 % for catalysts containing 16 at. % molybdenum.

In addition to the XPS data for O (1s), Zr (3d), and Mo (3d), the XPS data for C (1s) was also reported in Table 4-1. The presence of C (1s) was a result of atmospheric contamination and did not significantly change between catalysts.

5.2 Crystalline Structure (XRD)

The purpose of doing XRD analyses was to study the effect of molybdenum loading on the crystalline structure of the MoO_3-ZrO_2 catalysts. To infer what crystalline structures were present, the XRD patterns were compared to a standard cubic reference pattern (JCPDS file no. 27-997) and to results previously reported in the literature (Bhattacharyya et al., 2001).

Catalysts containing 9 to 16 at. % molybdenum closely resembled the standard cubic reference pattern, as can be seen in Figure 4-1. Many sources suggest that MoO_3-ZrO_2 catalysts exist in the metastable tetragonal phase at certain Mo-loadings. Calafat et al. (2000) stated that catalysts containing 10 to 50 at. % molybdenum were in the tetragonal phase, explaining that molybdenum opposes the tetragonal to monoclinic transition by decreasing the zirconia grains below a critical size and retarding the grain-growth rate. Zhao et al. (1997) noted that with sufficient Mo-loading, the XRD peaks for

MoO_3-ZrO_2 catalysts became broader, indicating that the ZrO_2 crystallite size was smaller and the MoO_3-ZrO_2 structures were tetragonal.

Catalysts containing less than 9 at. % molybdenum had additional characteristic monoclinic peaks at $2\theta = 28^{\circ}$ and $2\theta = 32^{\circ}$. Many authors have reported that pure zirconia exists primarily in the monoclinic phase with a small fraction existing in the tetragonal phase (Bhaskar et al., 2000 and Maity et al., 1999). One study showed that exposure to moist air was the reason for the existence of monoclinic zirconia. Xie et al. (2000) observed that ZrO_2 was tetragonal for treatment temperatures up to 600°C using Raman spectroscopy in dry air. When the same samples were exposed to moist ambient air during XRD analysis, monoclinic ZrO_2 was observed. According to Xie et al. (2000), the amount of molybdenum required to stabilize the zirconia grain structure in the tetragonal phase depends on the calcination temperature. At higher calcination temperatures, the amount of molybdenum required to hinder the tetragonal to monoclinic phase transition increases (Zhao et al., 1997).

The molybdenum loading where the monoclinic to cubic phase transition occurred in the present study was in agreement with a similar study conducted by Calafat et al. (2000). Calafat showed that the monoclinic to tetragonal phase transition occurred at around the same molybdenum loading (10 at. %) as the monoclinic to cubic phase transition in the present study (9 at. %). Even for catalysts prepared by wet impregnation, the Mo-loading where the phase transition occurred was around 10 at. %. Xie et al. (2000) observed that tetragonal ZrO_2 was present in catalysts containing 9 at. % molybdenum following treatment at 450-700°C. Zhao et al. (1997) noted a phase

transition from monoclinic to tetragonal between 3 and 14 at. % molybdenum for catalysts prepared by hydrogel impregnation and calcined at 450°C.

The XRD pattern for 19 at. % molybdenum was similar to the cubic reference pattern except for some peak broadening at $2\theta = 60^{\circ}$. This peak broadening could have been due to the formation of a new Mo-Zr phase. Calafat et al. (2000) speculated the formation of a new Mo-Zr phase for catalysts containing 50 at. % molybdenum through comparison of their XRD pattern with the JCPDS Powder Diffraction File for $Zr(MoO_4)_2$. A third reduction peak in the TPR profiles, likely due to the reduction of a different Mo phase, was also observed for catalysts containing 50 at. % molybdenum (Calafat et al., 2000). The exact molybdenum loading where the formation of a new Mo-Zr phase in the present and previous studies was subject to speculation. Highly dispersed MoO_3 crystallites having a size less than 4 nm, beyond the detection capacity of XRD, may have been present at lower Mo-loadings (Bhaskar et al., 2001).

The cubic lattice parameter did not change with molybdenum loading. According to Vegard's Law, the lattice parameter of a solid solution is directly proportional to the atomic percent of solute (Cullity, 1956). However, the atomic radii of molybdenum and zirconium are so close, 2.01 and 2.16 Å (Lide, 2004), that when zirconium ions are substituted by molybdenum ions, the lattice parameter does not change. The published lattice parameter for cubic zirconia is 5.09 Å (Walter et al., 2001), which is in good agreement with the calculated lattice parameter (5.10 ± 0.02 Å).

5.3 CO_2 Adsorption (DSC)

The purpose of measuring the isothermal heat of CO_2 adsorption was to determine the effect of Mo-loading on the strength of basic sites on the surface of MoO_3-ZrO_2 catalysts. Adsorption of CO_2 was studied at 100, 200, and 300°C using a DSC 111.

The strength of basic sites rapidly decreased with molybdenum loading for catalysts having a monoclinic crystalline structure, as can be seen by the 0.04 ± 0.01 J/m^2 drop in adsorption enthalpy at 100°C. For catalysts having a cubic structure (Mo/Zr = 0.11 to 0.16), the heat of adsorption decreased by 0.01 ± 0.004 J/m^2 at 100°C. These observations suggested that the strength of the basic sites was structure dependent.

Each catalyst was exposed to three doses of CO_2 at 100, 200, and 300°C, for a total of nine doses. The lower heats of adsorption with subsequent CO_2 injections showed that the adsorption process was not completely reversible. As the experiments were repeated at higher temperatures, the amount of irreversible adsorption decreased, indicating that more of the active sites were occupied. The irreversible adsorption was an indication of surface heterogeneity and the presence of different active sites (Groszek et al., 1998).

5.4 BET Surface Area

Adsorption of N_2 gas at 77 K was used to measure the BET surface area of ZrO_2-MoO_3 catalysts. The effect of Mo-loading on surface area was investigated in this study and a comparison between BET surface areas for catalysts prepared by co-precipitation, wet impregnation, and sol-gel impregnation was made for results previously reported in the literature.

In the present study, the surface area of MoO_3-ZrO_2 catalysts containing 0 to 16 at. % molybdenum increased with Mo-loading and then decreased. Calafat et al. (2000) observed a similar trend and stated that molybdenum decreased the sintering and grain-growth rate of ZrO_2, leading to higher surface areas up to a certain Mo-loadings. Many authors attribute the drop in surface area of MoO_3-ZrO_2 catalysts to the formation of a crystalline MoO_3 phase.

According to Calafat et al. (2000), stabilization of the ZrO_2 phase can be done in three different ways. Coating of ZrO_2 with a second oxide, such as MoO_3-, WO_3-, or CuO-, through wet-impregnation is one possible method. Another method is by the sol-gel method, which has been claimed superior over other methods (Calafat et al., 2000). Finally, co-precipitation of solid precursors, the method used in the present study, can be used to form a solid solution and stabilize ZrO_2 in the tetragonal or cubic phase.

The BET surface area values corresponding to different methods of preparation indicate that MoO_3-ZrO_2 catalysts prepared by co-precipitation or the sol-gel method exhibit a maximum surface area (S_{max}) with increasing Mo-loading followed by a decrease in surface area. Furthermore, catalysts prepared by the sol-gel method give higher S_{max} values than catalysts prepared by co-precipitation. As previously mentioned, the decrease in surface area after S_{max} is probably a result of the formation of a new crystalline MoO_3 phase. Calafat et al. (2000) and Zhao et al. (1997) observed that S_{max} depended on the calcination temperature. In both studies, S_{max} decreased with calcination temperature and occurred at lower Mo-loadings. Zhao et al. (1997) observed S_{max} values of 310, 224, 189, and 101 m^2/g for calcination temperatures of 450, 550, 600, and 750°C and Mo/Zr molar ratios of 0.27, 0.22, 0.22, and 0.14. Calafat et al. (2000) reported S_{max}

values of 116, 89 and 32 m^2/g for calcination temperatures of 500, 600, and 700°C and Mo/Zr molar ratios of 0.2 and 0.1.

According to Gopalan et al. (1995), the means by which the surface area of ZrO_2 decreases is through grain growth from 40-600°C and grain growth and phase transformation from 600-900°C. At these temperatures, the main mechanism by which sintering and grain growth occur is through surface diffusion (Gopalan et al., 1995). The surface area results for catalysts prepared by co-precipitation or the sol-gel method confirm that molybdenum reduces the sintering rate of ZrO_2.

MoO_3-ZrO_2 catalysts prepared by wet-impregnation yielded lower surface areas that decreased with molybdenum loading (Li et al., 1999 and Maity et al., 1999). Maity et al. (1999) speculates that preparation by wet-impregnation causes blockage of the pore mouth with molybdenum oxide, leading to a lower surface areas.

Calafat et al. (2000) reported BET surface areas that were similar to those obtained in the present study for catalysts prepared by co-precipitation and calcined at 500°C. Surface areas obtained by Calafat et al. (2000) for catalysts containing 10 and 20 at. % molybdenum were 100 and 116 m^2/g. In the present study, catalysts containing 11 and 19 at. % molybdenum had surface areas of 101 and 111 m^2/g. Other studies that used the same method of catalyst preparations did not give such comparable results. Especially notable is the wide range of values reported for the surface area of pure zirconia, which should mainly depend on the calcination temperature and not the method of catalyst preparation. Zhao et al. (1997), Bhaskar et al. (2000), and the author of the present study reported BET surface area values of 52, 96, 84 and 20 ± 0.9 m^2/g for pure ZrO_2 calcined between 450 and 550°C.

5.5 Temperature Programmed Reduction (TPR)

TPR was done to study the effect of Mo-loading on the reducibility of MoO_3-ZrO_2 catalysts. The amount of hydrogen uptake and the temperature of reduction were obtained from the TPR spectra using peak fitting software.

The TPR profiles (Figure 4-4) showed that pure ZrO_2 was not reducible up to 500°C. In a study conducted by Bhaskar et al. (2000), no reduction peaks were observed up to 1000 °C for pure ZrO_2 calcined at 500°C. Maity et al. (1999) observed a broad reduction peak for a commercial (Harshaw) zirconia support at 726°C without giving a reason for this peak or the sample history. In the present study, the catalysts were not reduced beyond their calcination temperature of 500°C to avoid additional structural changes.

Catalysts containing 3 at. % molybdenum showed a one-peak spectrum that transformed to a two-peak spectrum at 5 at. % molybdenum. With further molybdenum loading, the two peaks became more pronounced and shifted to lower temperatures, suggesting that reduction occurred in two stages and the catalysts were more reducible. Calafat et al. (2000) also observed that the reduction of MoO_3-ZrO_2 catalysts occurred in two stages. The low temperature peak (T = 416°C, Mo/Zr = 0.1) was assigned to the reduction of dispersed polymolybdates and the high temperature peak (T = 660°C, Mo/Zr = 0.1) was assigned to the reduction of MoO_3 to MoO_2 (Calafat et al., 2000). Bhaskar et al (2001) found that reduction of MoO_3 to MoO_2 occurred at around 767°C while reduction of MoO_2 to Mo occurred at around 987°C. The peaks observed for the reduction of MoO_3 to MoO_2 by Calafat et al. (2000) may have been lower because of Zr-O/Mo-O interactions, owing to the method of catalyst preparation (co-precipitation).

Temperature programmed reduction profiles of MoO_3-ZrO_2 catalysts shown in other studies were considerably different from those observed in the present study. According to Bosch et al. (1984), comparing TPR spectra obtained by different investigators is difficult because of the experimental conditions differing in H_2 concentration, flow rate, heating rate, sample size, and pretreatment. Furthermore, a quantitative approach towards comparing TPR profiles of catalysts prepared by different techniques is difficult. In a study conducted by Calafat et al. (2000), catalysts were prepared by co-precipitation and calcined at 500°C. Temperature programmed reduction was carried out at a heating rate of 20°C, resulting in reduction peaks that occurred at higher temperatures and were better resolved than those in the present study. The dependence of heating rate on reduction profiles has been described by Jones et al. (1986). In a study involving the reduction of nickel oxide, increasing the heating rate from 0.09 to 0.31 K/s caused the peak temperature to increase by 33 K (Jones et al., 1986). Comparing the results from the present and previous study, Calafat et al. (2000) observed a reduction peak (Mo/Zr = 0.10, heating rate = 20°C/min) that was 59 K higher than the first reduction peak in the present study (Mo/Zr = 0.11, heating rate = 10°C/min). Bosch et al. (1984) observed that better resolution and additional peaks occurred at higher heating rates for the reduction of V_2O_5. Calafat et al. (2000) found that for a catalyst containing 10 at. % molybdenum, the first and second reduction peaks were separated by 240°C. In the present study, the peaks for a catalyst containing 11 at. % molybdenum were only separated by 38°C.

Another factor that influenced the reduction profiles of MoO_3-ZrO_2 catalysts was the method of preparation. Two peaks were observed for catalysts prepared by incipient

wetting of ZrO_2 calcined at 500°C in a study conducted by Bhaskar et al. (2000). Peak assignment was done based on the geometry of the MoO_3 species. Low temperature peaks at 400 – 450°C (Mo/Zr = 0.01-0.08) were assigned to the reduction of octahedral species whereas high temperature peaks at 700 - 830°C were assigned to the reduction of tetrahedral species. Maity et al. (2000) interpreted the MoO_3-ZrO_2 reduction profiles in a similar way for catalysts prepared by incipient wetting of a commercial Harshaw support calcined at 450°C. The low temperature peak (542°C) observed at 2 at. % Mo-loading was assigned to the reduction of octahedral species and the high temperature peak (621°C) was assigned to the reduction of tetrahedral species (Maity et al., 2000). Peak assignment based on MoO_3 geometry was not done in the present study because the catalysts consisted of a solid solution of molybdenum and zirconium.

Independent of the method of catalyst preparation, the total hydrogen uptake increased with Mo-loading. Catalysts prepared by incipient wetting of ZrO_2 gave low and high temperature peak areas that increased from 0.1739 to 1.8315 a.u. and 0.3200 to 4.1404 a.u., respectively, as the Mo-loading was increased from 1 to 8 at. % (Bhaskar et al., 2001). Qualitatively, the peak areas for catalysts prepared by incipient wetting of a commercial Harshaw support increased as the Mo-loading increased (Maity et al., 2000). In the present study, the total area under the TPR profiles or hydrogen uptake increased with molybdenum content, indicating that the catalysts were more reducible at higher Mo-loadings.

The effect of crystalline structure on hydrogen uptake could be seen by the different trend lines shown in Figures 4-5 and 4-6. In Figure 4-5, where hydrogen uptake per m^2 catalyst was plotted as a function of Mo-loading, two distinct linear trend lines

corresponding to the monoclinic and cubic regions were fit to the data. A trend line with a slope approximately equal to 1 was fit to the monoclinic region while a trend line with a slope closer to 0.2 was fit to the cubic region. In Figure 4-6, where the hydrogen uptake per g catalyst as a function of Mo-loading was shown, a linear trend line was fit to the entire data set. The dependence of hydrogen uptake on crystalline structure showed that in the cubic region, the Mo-O-Zr interactions were not as strongly effected by the Mo-loading as in the monoclinic region. Increasing the Mo-content from 0 to 5 at. % in the monoclinic region increased the hydrogen uptake by 5.9 mL/m^2_{cat}. In the cubic region, increasing the Mo-content from 9 to 16 at. % increased the hydrogen uptake by 1.1 mL/m^2_{cat}.

All of the TPR experiments were repeated at least twice. Some repeated runs were done using a fresh sample while others were oxidized in between treatments. In both cases, the same TPR profiles were obtained. The maximum differences in hydrogen uptake found by integrating the low and high temperature peaks were 1.82 and 0.26 mL/g_{cat}, respectively (Mo/Zr = 0.16). Low and high temperature peaks differed by a maximum of 41 and 77°C, respectively (Mo/Zr = 0.05). For the total hydrogen uptake, the maximum difference in hydrogen uptake was 1.78 mL/g_{cat} (Mo/Zr = 0.05). The slight differences associated with the hydrogen uptake and peak temperatures were attributed to the subjective nature of peak fitting.

5.6 Temperature Programmed Oxidation (TPO)

Temperature programmed reduction was done to determine if the TPR process was reversible. Temperature programmed oxidation profiles of MoO_3-ZrO_2 showed that

the oxygen uptake increased with Mo-content in the same way as the hydrogen uptake increased. Catalysts that were subjected to temperature programmed reduction following TPO gave the same reduction profiles as untreated samples subjected to TPR. The TPR results prior to and following treatment with TPO suggested that reduced catalysts returned to their unreduced state following oxidation.

5.7 Temperature Programmed Desorption (TPD)

The acid properties of MoO_3-ZrO_2 catalysts were investigated using ammonia (NH_3) temperature programmed desorption. According to Auroux et al. (2001), the activity and selectivity of metal oxides is related to their acid-base properties. The two main techniques for characterizing the acidity of surfaces are the indicator titration method and the gas-phase adsorption method (Carniti et al., 1994). Different probe molecules can be used, based on their basicity and molecular size, and both Brønsted and Lewis sites can be investigated using the gas-phase adsorption method. Ammonia was used as a probe molecule in the present study because of its strong basic strength (pKa = 9.2), stability, and small size (Bhaskar et al., 2001).

The TPD profiles (Figure 4-8) showed that the acidic sites were distributed in two regions corresponding to moderate and strong acid sites. As can be seen by the increasing area under the curves, the number acid sites increased with Mo-loading. Irrespective of Mo-loading, the first and second peaks occurred at around 150°C and 300°C, respectively. The total volume of ammonia desorbed per unit mass and unit surface area were calculated from the peak area. The volume of ammonia desorbed per unit surface area decreased and then increased with increasing Mo-loading, owing to the

increasing surface area up to 16 at. % molybdenum. The effect of crystallite structure on acidity was apparent in both Figure 4-9 (Volume of NH_3 desorbed per unit mass) and Figure 4-10 (Volume of NH_3 desorbed per unit surface area). Figure 4-9 showed a break in the linear trend where the monoclinic to cubic phase transformation took place (Mo/Zr = 0.05). Figure 4-10 showed that the volume of ammonia desorbed rapidly decreased in the monoclinic region (Mo/Zr = 0 - 0.5), stayed constant in the cubic region (Mo/Zr = 0.11 - 0.16) , and then increased at 19 at. % molybdenum.

According to Li et al. (1999), MoO_3-ZrO_2 catalysts are weak acids compared to other solid acids. Li et al. (1999) report peaks of NH_3 desorption at 327°C (SiO_2-Al_2O_3), 377°C (H-ZSM-5), 427°C (mordenite), and 557°C ($Cs_{2.5}H_{0.5}PW_{12}O_{40}$). However, comparing NH_3 TPD results obtained by different investigators is difficult. Bhaskar et al. (2001) observed two NH_3 TPD peaks at 300 and 550°C that increased in intensity with increasing Mo-loading for catalysts prepared by incipient wetting of ZrO_2 and calcined at 500°C. Higher peak temperatures observed by Bhaskar et al. (2001) compared to those observed in the present study could have been due to the catalyst preparation technique or the sample size (200 mg). Li et al (1999) observed a single adsorption peak around 200°C for catalysts prepared by impregnation of $Zr(OH)_4$ and calcined at temperatures from 300 to 900°C. Dosing the catalysts with ammonia at a higher temperature (100°C) may have been responsible for the lower desorption temperature that was observed. Because of the different TPD procedures that were employed, comparing the results from different studies or concluding which catalyst preparation technique gave the highest surface acidity, impregnation of $Zr(OH)_4$ (Li et al., 1999), incipient wetting of ZrO_2 (Bhaskar et al., 2001), or co-precipitation, was not possible.

Various studies have found that as the surface acidity increases, the catalyst activity and selectivity increases. Baskar et al. (2001) found that as the number of strong acid sites increased, the conversion of 3-picoline and the selectivity towards nicotinonitrile increased. Li et al. (1999) concluded that the catalytic activity of MoO_3-ZrO_2 for water-concerning reactions were governed partly by the acidic properties of the surface. As the calcination temperature was increased, the conversion in esterification and the density of NH_3 adsorbed on the surface increased (Li et al., 1999). Tanabe (1985) reported that high catalytic activities and selectivities of ZrO_2-MoO_3 catalysts were explained by the interaction of weakly acidic sites with moderately basic sites. In the present study, the highest conversion of methyl-cyclopentane occurred at a Mo-loading of 3 at. %, corresponding to the highest acid density of the reducible catalysts.

5.8 Ring-Opening Reaction

Methyl-cyclopentane (mcp) was used as a probe molecule to study conversion over MoO_3-ZrO_2 catalysts. According to McVicker et al. (2002), petroleum distillates contain a complex mixture of five and six membered napthenes containing multiple alkyl substituents which are joined or fused to each other. Albertazzi et al. (2003) states that straight-run stocks typically contain 20 - 40 vol.% aromatics while cracked stocks contain 40 - 70 vol.%. Probe molecules, consisting of pure compounds, give useful insight into the reaction mechanism before complex feed stocks are studied. Methyl-cyclopentane was chosen as a probe molecule in this preliminary reaction study because its ring opening rate is one to two orders faster than alkylcyclohexanes, owing to the higher ring

strain of five-membered rings (6 - 7 kcal/mol) compared to six-membered rings (1 kcal/mol) (McVicker et al., 2002).

Maity et al. (2000) does not predict further improvement of traditional hydrotreating catalysts, such as Al_2O_3. Instead, the development of a new catalyst, such as ZrO_2, seems to be the only solution. ZrO_2-MoO_3 catalysts have shown significant promise as hydrotreating catalysts, owing to their acid-base properties, thermal stability, and extreme hardness, compared to classical catalysts such as alumina or silica (Bhaskar et al., 2000). Previous investigators have shown that the yield of alkanes over conventional hydrocracking catalysts is low because of dealkylation and secondary cracking (McVicker et al., 2002). In a study conducted by McVicker et al. (2002), mcp reacted over Pt/Al_2O_3 showed a selectivity towards n-hexane of 0.41 ($T = 350^{\circ}C$, $P = 2.85$ MPa). In the present study, measuring the selectivity towards n-alkanes was not possible because of the complex mass spectra of hydrocarbons. Instead, the conversion of mcp was measured by monitoring the most abundant m/z ratio of mcp (41). Consistent with what has been reported by Bhaskar et al. (2001), the disappearance of mcp was greatest for the catalyst with the highest acidity ($Mo/Zr = 0.03$).

Ring-opening reactions have been reported to occur via two independent mechanisms: the direct route, involving bifunctional catalysts, and the two-stage route, involving hydrogenation followed by reaction over monofunctional catalysts. According to McVicker et al. (2002), combining an acidic function with a high-activity hydrogenolysis metal (group VIII metals) results in a bifunctional catalyst that outperforms conventional hydrotreating catalysts. The proposed ring-opening mechanism on metal-free acidic zeolites is referred to as non–classical Haag-Dessau

mechanism, where alkanes are directly protonated to non-classical carbonium ions in the transition state. Weitkamp et al. (2001) reports that yields of C_{2+}-n-alkanes of methylcyclohexane over H-ZSM-5 (n_{Si}/n_{Al} = 20) are comparable to those during the conversion of toluene on Pd/H-ZSM-5 (ca. 72%) under a high excess of hydrogen ($pH_2/pM\text{-}CH_x \sim 100$), high temperature (400°C), and high pressure (6 MPa).

Work done by Weitkamp et al. (2001) suggests that higher conversions should have been observed in the present study. Higher conversions may have been achieved if higher reaction pressures and temperatures were employed. Weitkamp et al. (2001) states that napthenic rings are mostly opened at 3-5 MPa and 260-400°C. Albertazzi et al. (2003) reports that increasing the pressure from atmospheric to 6 MPa significantly increases the catalytic activity of noble-metal-containing (Rh, Pd, Pt, or Ir) mesoporous MCM-41 catalysts. Teschner et al. (2000) observed a monotonic increase in turnover frequency of mcp as the hydrogen pressure was increased from 100 to 500 Torr over Al_2O_3 catalysts containing various Rh-loadings. Due to instrumental constraints, the reactions were carried out at atmospheric pressure ($\approx$95 - 99 kPa).

CHAPTER 6 CONCLUSION

6.1 Conclusion

It has been shown that pure zirconia exists in the monoclinic phase and that incorporation of molybdenum promotes a phase transition to the cubic phase. The phase transition occurs at 9 at.% molybdenum, at which molybdenum decreased the zirconia grains below a critical size and retarded the grain growth rate. At 19 at. % molybdenum, peak broadening in the XRD patterns and a decrease in surface area was observed, providing evidence for the formation of new Mo-Zr phase.

The surface area of MoO_3-ZrO_2, as measured by the BET method, increased with Mo-loading up to 16 at. % and then decreased. The increase in surface area was attributed to the ability of molybdenum to stabilize ZrO_2 grains below a certain size and prevent grain growth. Beyond 16 at. % molybdenum, the decrease in surface area was attributed to the formation of a new MoO_3 phase, in accordance with the XRD results.

The strength of basic sites, as measured by CO_2 adsorption, decreased with increasing molybdenum loading. Catalysts having a monoclinic cubic structure showed a faster decrease in basic strength than those with a cubic structure, suggesting that the surface basicity was structure dependent. Subsequent doses of CO_2 showed that the adsorption process was not entirely reversible, owing to the presence of different active sites.

Pure zirconia was not reducible up to 500°C. With the addition of molybdenum, the catalysts became more easily reduced. Two reduction peaks were observed for

catalysts containing 5 to 19 at. % molybdenum. Oxidation of the catalysts following reduction showed that the reduction process was completely reversible.

The acidic sites of the MoO_3-ZrO_2 catalysts, as measured by temperature programmed desorption of ammonia, were distributed in two regions corresponding to moderate and strong acid sites. The volume of ammonia desorbed per unit surface area rapidly decreased in the monoclinic region, remained relatively constant in the cubic region, and then increased at 19 at. % molybdenum, indicating that the crystalline structure had an effect on the surface acidity. Based on catalyst mass, the number of acid sites increased with increasing molybdenum loading. Consistent with what has been reported regarding the effect of acidity on catalytic activity, the conversion of methyl-cyclopentane was the greatest for the catalyst with the highest acidity (Mo/Zr = 0.03).

6.2 Future Work

Much future work involving the MoO_3-ZrO_2 catalysts that were investigated in this study is anticipated. A more extensive study involving their ring-opening selectivity and activity towards C6 alkanes will be done using other model compounds (methyl-cyclohexane and cyclohexane).

An attempt to enhance the ring-opening activity of MoO_3-ZrO_2 catalysts will be made by incorporating iridium. The resulting bifunctional Ir/MoO_3-ZrO_2 catalysts will be characterized using the same techniques as in the present study. In addition to the incorporation of iridium, promoters (Ni, Co) will be added to the catalysts and their ability to inhibit side reactions will be investigated. After the bifunctional catalysts have

been assessed using model compounds, their performance will be evaluated using real heavy gas oil feedstocks.

REFERENCES

S. Albertazzi, R. Ganzerla, C. Gobbi, M. Lenarda, M. Mandreoli, E. Salatelli, P. Savini, L. Storaro, and A. Vaccari, "Hydrogenation of naphthalene on noble-metal-containing mesoporous MCM-41 aluminosilicates", Journal of Molecular Catalysis 200 (2003) 261-270.

W. Alvarez and D. Resasco, "Methylcyclopentane Ring Opening as a Reaction Test for Pt Catalysts Supported on Non-acidic Materials", Journal of Catalysis 164 (1996), 467-476.

A. Auroux, R. Monaci, E. Rombi, V. Solinas, A. Sorrentino, and E. Santacesaria, "Acid sites investigation of simple and mixed oxides by TPD and microcalorimetric techniques", Thermochimica Acta 379 (2001), 227-231.

AutoChem II 2920 Automated Catalyst Characterization System Operator's ManualV2.00, Norcross, GA (2003).

S. Bhattacharyya, S.K. Pratihar, R.K. Sinha, R.C. Behera, and R.I. Ganguly, "Preparation of alumina-high zirconia microcomposite by combined gel-precipitation," Materials Letters 53 (2001) 425-431.

C. Berger, A. Raichle, R.R. Rakoczy, Y. Traa, and J. Weitkamp, "Hydroconversion of methylcyclohexane on TEOS-modified H-ZSM-5 zeolite catalysts: Production of a high-quality synthetic steamcracker feedstock", Microporous and Mesoporous Materials 59 (2003) 1-12.

T. Bhaskar, K. R. Reddy, C.P. Kumar, M.R.V.S. Murthy, and K.V.R. Chary, "Characterization and reactivity of molybdenum oxide catalysts supported on zirconia", Applied Catalysis 211 (2001) 189-201.

H. Bosch, B.J. Kip, J.C. van Ommen, and P.J. Gellings, "Factors Influencing the Temperature-programmed Reduction Profiles of Vanadium Pentoxide", J. Chem. Soc. Faraday I 80 (1984) 2479-2488.

D. Briggs, and M.P Seah, *Practical Surface Analysis (Second Edition)*, John Wiley & Sons Ltd., New York (1990).

A. Calafat, L. Avilán, and J. Aldana, "The influence of preparation conditions on the surface area and phase formation of MoO_3/ZrO_2 catalysts", Applied Catalysis 201 (2000) 215-223.

P. Carniti, A. Gervasini, and A. Auroux, "Energy Distribution of Surface Acid Sites of Metal Oxides", Journal of Catalysis 150 (1994), 274-283.

A. Corma, V. González-Alfaro, and A.V. Orchillés, "Decalin and Tetralin as Probe Molecules for Cracking and Hydrotreating the Light Cycle Oil", Journal of Catalysis 200 (2001) 34-44.

B.D. Cullity, *Elements of X-Ray Diffraction*, Addison-Wesley, Reading, MA (1956).

Dycor Quadrupole Gas Analyzer Operating Instructions for models: M100, MA100, M200, MA200, M100M, MA10M, M200M, MA200M, Pittsburgh, PA. (1994).

J.L. Falconer, "Temperature-Programmed Desorption and Reaction: Applications to Supported Catalysts", Catal. Rev. –Sci. Eng 25 (2) (1993) 141-227.

R. Gopalan, C.-H. Chang, and Y.S. Lin, "Thermal stability improvement on pore and phase structure of sol-gel derived zirconia", J. Mater, Sci 30 (1995) 3075-3081.

A.J. Groszek, "Flow adsorption microcalorimetry", Thermochimica Acta 312 (1998), 133-143.

A. Jones, and B.D. McNicol, *Temperature-Programmed Reduction for Solid Materials Characterization*, Heinz Heinemann Inc., Berkeley, California (1986).

L. Li, Y. Yoshinaga, and T. Okuhara, "Unprecedented acceleration effects of water on acid-catalyzed reactions over molybdena-zirconia catalysts", Catalysis Letters 83 (2002), 231-243.

S.K. Maity, M.S. Rana, B.N. Srinivas, S.K. Bej, G. M. Dhar, and T.S.R. Prasada, "Characterization and evaluation of ZrO_2 supported hydrotreating catalysts", Journal of Molecular Catalysis 153 (2000) 121-127.

G.B. McVicker, M. Daage, M.S. Touvelle, C.W. Hudson, D.P. Klein, W.C. Baird, B.R. Cook, J.G. Chen, S. Hanter, D.E.W. Vaughan, E.S. Ellis, and O.C. Feeley, "Selective Ring Opening of Naphthenic Molecules", Journal of Catalysis 210 (2002) 137-148.

E. W. Nuffield, *X-Ray Diffraction Methods*, John Wiley & Sons, Inc., New York (1996).
Setaram DSC 111 Operating Manual, France (2000).

A. Raichle, Y. Traa, and Jens Weitkamp, "Preparation of a high-quality synthetic steamcracker feedstock from methylcyclohexane on acidic zeolite H-ZSM-5: influence of the hydrogen partial pressure", Applied Catalysis 41 (2003), 193-205.

B.M. Reddy, and V.R. Reddy, "Influence of SO_4^{2-}, Cr_2O_3, MoO_3, and WO_3 on the stability of ZrO2-tetragonal phase", Journal of Materials Science Letters 19 (2000) 763-765.

G. A. Somorjai, *Introduction to Surface Chemistry and Catalysis*, John Wiley & Sons, Inc., New York (1994).

K. Tanabe, "Surface and Catalytic Properties of ZrO_2", Materials Chemistry and Physics 13 (1985) 347-364.

D. Teschner, K. Matusek, and Z. Paál, "Ring Opening of Methylcyclopentane on Alumina Supported Rh Catalystss of Different Metal Loading", Journal of Catalysis 192 (2000), 335-343.

G.D. Ulrich, *A Guide to Chemical Engineering Reactor Design and Kinetics*, Braun-Brumfield, Inc., Durham, New Hampshire (1993).
H.S. Lipson, *Crystals and X-rays*, Wykeham Publications (London) Ltd, London and Winchester (1970).

E.J. Walter, S.P. Lewis, and A.M. Rappe, "First Principles Study of Carbon Monoxide adsorption on Zirconia Supported Copper", Surface Science 495 (2001), 44-50.

J. Weitkamp, A. Raichle, and Y. Traa, "Novel zeolite catalysis to create value from surplus aromatics: preparation of C2+-n-alkanes, a high-quality synthetic steamcracker feedstock", Applied Catalysis 222 (2001) 277-297.

S. Xie, K. Chen, A. T. Bell, and E. Iglesia, "Structural Characterization of Molybdenum Oxide Supported on Zirconia", J. Phys. Chem. 104 (2000), 10059-10068.

B. Zhao, X. Xu, H. Ma, D. Sun, and J. Gao, "Monolayer dispersion of oxides and salts on surface of ZrO_2 and its application in preparation of ZrO_2-supported catalysts with high surface areas", Catalysis Letters 45 (1997) 237-244.

Y. Zhuang and A. Frennet, "Hydrogen Effect on Hydrocarbon Reactions over Bulk Tungsten Carbide", Journal of Catalysis 163 (1996), 223-231.